Palacký University, Olomouc

Bachelor thesis

Olomouc 2023 **Karolína Hrabáková**

Palacký University, Olomouc

Faculty of Science

Department of Cell Biology and Genetics

Profiling of oxidation products during differentiation in human cell lines

Bachelor thesis

Karolína Hrabáková

Study programme: Biology

Study Specialization: Molecular and Cellular Biology

Form of study: Full-time

Olomouc 2023 **Supervisor: doc. Ankush Prasad, Ph.D.**

UNIVERZITA PALACKÉHO V OLOMOUCI

Přírodovědecká fakulta

Akademický rok: 2021/2022

ZADÁNÍ BAKALÁŘSKÉ PRÁCE

(projektu, uměleckého díla, uměleckého výkonu)

Jméno a příjmení:	**Karolína HRABÁKOVÁ**
Osobní číslo:	**R20698**
Studijní program:	**B1501 Biologie**
Studijní obor:	**Molekulární a buněčná biologie**
Téma práce:	**Profilování oxidačních produktů během diferenciace lidských buněčných linií**
Zadávající katedra:	**Katedra buněčné biologie a genetiky**

Zásady pro vypracování

1. Posouzení literatury na téma biomolekulární oxidace
2. Obeznámení se s přípravou vzorků, standardizací a používáním spektroskopických metod
3. Vypracování stručného přehledu reakčních mechanismů vedoucích k biomolekulární oxidaci
4. Zhodnocení naměřených výsledků a jejich porovnání s literaturou
5. Připravení bakalářské práce

Rozsah pracovní zprávy:
Rozsah grafických prací:
Forma zpracování bakalářské práce: **tištěná**
Jazyk zpracování: **Angličtina**

Seznam doporučené literatury:

Halliwell B., Gutteridge J. M. C. (2007). Free Radicals in Biology and Medicine, 4th Edn. New York, NY: Oxford University Press.
Chanput W, Mes JJ, Wichers HJ (2014) THP-1 cell line: An in vitro cell model for immune modulation approach. International Immunopharmacology 23: 37-45
Kumar A, Prasad A, Sedlářová M, Pospíšil P (2019) Organic radical imaging in plants: Focus on protein radicals. Free Radic Biol Med 130: 568-575.
Mason RP (2016) Imaging free radicals in organelles, cells, tissue, and in vivo with immuno-spin trapping. Redox Biol 8: 422-429.
Pospíšil P, Prasad A, Rac M (2019) Mechanism of the Formation of Electronically Excited Species by Oxidative Metabolic Processes: Role of Reactive Oxygen Species. Biomolecules 9.

Vedoucí bakalářské práce: **Mgr. Ankush Prasad, Ph.D.**
Katedra biofyziky

Datum zadání bakalářské práce: **29. března 2022**
Termín odevzdání bakalářské práce: **31. července 2023**

L.S.

doc. RNDr. Martin Kubala, Ph.D.
děkan

prof. RNDr. Zdeněk Dvořák, DrSc.
vedoucí katedry

V Olomouci dne 6. dubna 2022

BIBLIOGRAPHICAL IDENTIFICATION

Author's name	Karolína Hrabáková
Title	Profiling of oxidation products during differentiation in human cell lines
Type of thesis	Bachelor
Department	Cell Biology and Genetics, Faculty of Science UP, Olomouc
Supervisor	doc. Ankush Prasad, PhD
The year of defence	2023

Summary

U-937 is a promonocytic cell line, which can differentiate when met by a stimulus to macrophages or dendritic cells. During differentiation, reactive oxygen species are formed as a by-product. In this bachelor thesis, my aim was to understand whether the formed reactive oxygen species damage the differentiated cells. Confocal laser scanning microscopy (CLSM) and western blotting (specifically immunoblotting) using anti-MDA and anti-NOX4 antibodies were used for the experiments. Phorbol 12-myristate 13-acetate (PMA) was used as the differentiation agent. In this study and based on results reported in the thesis, we conclude that the differentiation process was a dose-dependent process and high concentration is coupled with cell apoptosis in addition to differentiation. From the confocal images and western blotting analyses, it can be concluded that despite differentiation in cells, both the expression of NOX4 and the oxidized NOX4 subunit in the cytoplasm is higher with increasing concentration of PMA.

Keywords	U-937, reactive oxygen species, NADPH oxidase, monocyte differentiation
Number of pages	65
Number of appendices	0
Language	English

BIBLIOGRAFICKÉ ÚDAJE

Jméno autora	Karolína Hrabáková
Titul	Profilování oxidačních produktů během diferenciace lidských buněčných linií
Typ práce	Bakalářská
Pracoviště	Katedra buněčné biologie a genetiky, PrF UP v Olomouci
Vedoucí	doc. Ankush Prasad, PhD
Rok obhajoby práce	2023

Souhrn

U-937 je promonocytická buněčná linie, která se pomocí stimulu dále může diferenciovat na makrofágy nebo dendritické buňky. Při diferenciaci se jako vedlejší produkt tvoří reaktivní formy kyslíku. V této bakalářské práci se snažím zjistit, jestli vytvořené reaktivní formy kyslíku při diferenciaci buňky poškozují. Pro experimenty byly použity metody konfokální laserové skenovací mikroskopie (CLSM) a western blotting (specificky immunoblotting) s anti-MDA a anti-NOX4 protilátkami. Buňky byly diferenciované pomocí forbol-12-myristát-13-acetátu (PMA). V této studii spolu s výsledky této práce bylo zjištěno, že proces diferenciace je závislý na podané dávce látky a vysoká koncentrace PMA je spojená s buněčnou apoptózou spolu s diferenciací. Z konfokálních fotografií a western blotting analýz bylo zjištěno, že i přes diferenciaci je množství exprese NOX4 a množství oxidované NOX4 podjednotky přítomné v cytoplazmě při stoupajících koncentracích PMA vyšší.

Klíčová slova	U-937, reaktivní formy kyslíku, NADPH oxidáza, monocytická diferenciace
Počet stran	65
Počet příloh	0
Jazyk	Angličtina

DECLARATION

I declare that I developed this bachelor thesis separately by showing all the sources and authorship. I agree with the publication of the thesis by Act no. 111/1998 Coll., about universities, as amended. I was aware of the rights and obligations arising from the Act no. 121/2000 Coll., the Copyright Act, as amended, are applied to my work.

In Olomouc …… ……..……

ACKNOWLEDGEMENT

I would like to thank the supervisor of my thesis, doc. Ankush Prasad, Ph.D., for all the time he has spent with me, invested in me, and helped me during my thesis writing and experiments. I would also like to thank M.Sc. Renuka R Manoharan, Ph.D., M.Sc. Deepak Rathi and all members of the Department of Biophysics, Faculty of Science, Palacký University, Olomouc that helped me when it was needed. I am also grateful for the help of doc. RNDr. Michaela Sedlářová, Ph.D., Department of Botany, Palacký University. Also thank you to everyone around me including my family and friends, who really helped me during the tough times of the last three years. I would like to thank the grant that my work has been overseen by the IGA project (IGA_PrF_2023_023).

CONTENTS

ABBREVIATIONS

AA	Ascorbic acid
ADSC	Adipose derived stem cell
APC	Antigen presenting cell
APS	Ammonium persulfate
BCA	Bicinchoninic acid
BIS	N, N´-Methylene-Bis-Acrylamide
BSA	Bovine serum albumin
CBB	Coomassie® Brilliant Blue G-250
CLSM	Confocal laser scanning microscopy
CNS	Central nervous system
CPC	Cardiac precursor cell
CSF-1	Colony stimulating factor 1
DC	Dendritic cells
DMSO	Dimethyl sulfoxide
DTT	Dithiothreitol
DUOX1	Dual nicotinamide adenine dinucleotide phosphate oxidase 1
DUOX2	Dual nicotinamide adenine dinucleotide phosphate oxidase 2
DUOXA1	Dual nicotinamide adenine dinucleotide phosphate oxidase activator 1
DUOXA2	Dual nicotinamide adenine dinucleotide phosphate oxidase activator 2
ER	Endoplasmic reticulum
$FADH_2$	Flavine adenine dinucleotide
FBS	Foetal bovine serum
GM-CSF	Granulocyte-macrophage colony stimulating factor

GTP	Guanosine triphosphate
HNE	4-Hydroxy-2-trans-nonenal
$HO^{\bullet}$	Hydroxyl radical
$HO_2^{\bullet}$	Hydroperoxyl radical
$HOCl^{-}$	Hypochlorous acid
HRP	Horseradish peroxidase
IL-4	Interleukin 4
LPS	Liposaccharides
MAP	Mitogen-activated protein
MDA	Malondialdehyde
NADPH	Nicotinamide adenine dinucleotide phosphate
NC	Negative control
NCSC	Neutral crest stem cell
NOX	Nicotinamide adenine dinucleotide phosphate oxidase
NOX2	Nicotinamide adenine dinucleotide phosphate oxidase 2
NOX1	Nicotinamide adenine dinucleotide phosphate oxidase 1
NOX3	Nicotinamide adenine dinucleotide phosphate oxidase 3
NOX4	Nicotinamide adenine dinucleotide phosphate oxidase 4
NOX5	Nicotinamide adenine dinucleotide phosphate oxidase 5
NOXA1	Nicotinamide adenine dinucleotide phosphate oxidase activator 1
NOXO1	Nicotinamide adenine dinucleotide phosphate oxidase organiser 1
$O_2^{\bullet-}$	Superoxide anion radical
PC	Positive control
PKC	Protein kinase C

PMA	Phorbol-12-myristate-13-acetate
PNS	Peripheral nervous system
PUFA	Polyunsaturated fatty acid
$R^{\bullet}$	Carbon centred radical
RH	Species with a methylene group
ROS	Reactive oxygen species
$RO^{\bullet}$	Alkoxyl radical
$RO_2^{\bullet}$	Peroxyl radical
ROOH	Organic hydroperoxide
RS	Reactive species
SOD	Superoxide dismutase
TF	Transcriptional factor
TPA	12-O-tetradecanoylphorbol-13-acetate
TRADD	TNFR1-associated death domain protein
VD3	1,25-dihydroxy vitamin D3
VSMC	Vascular smooth muscle cell
X	Reactive species
XH	Non-reactive species

LIST OF FIGURES

LIST OF TABLES

1. INTRODUCTION

Reactive oxygen species (ROS) is a term widely used for molecules derived from oxygen (Li *et al*., 2016). These ROS then must be processed, because they can cause huge damage to the differentiated cell if not regulated. Several cascades were developed in cells to make sure that excess of ROS generated is properly processed. Reactive oxygen species however also have a role in cell signaling like gene expression and other important functions. One of the enzymes that process the ROS is Nicotinamide adenine dinucleotide phosphate oxidase also referred to as NADPH oxidases, which forms superoxide anion radicals ($O_2^{\bullet-}$) and eventually H_2O_2. The NADPH oxidases are a family of enzyme complexes, each present in various parts of an organism. We know, that 4 out of the 7 NADPH oxidases are present in phagocytes (Lee *et al*., 2014; Maitra *et al*., 2009; Marzaioli *et al*., 2017), thus our aim in this study is to add to the understanding of differentiation and changes in expression and/or its relation with biomolecule oxidation in human cells.

During monocyte-to-macrophage differentiation, ROS are formed as a by-product and processed. An imbalance in production and scavenging activity by endogenous antioxidants is known to be responsible for oxidative damage. To address and characterize the protein likely to be damaged is addressed within the frame of the study. This study also shed some light on whether too much of differentiating agent can lead to apoptosis besides cell differentiation.

U-937 is a promonocytic cell line able to differentiate into either macrophage-like or dendritic cell-like morphologies (Stephens *et al*., 2008; Sundström & Nilsson, 1976). It is widely used nowadays for profiling macrophage differentiation studies next to the THP-1 cell line. It is reliable because of its uniformity in behaviour. The cell line does not have a Hayflick limit, which makes it easier to work with. The differentiation agent widely used for these cell lines is PMA, next to 12-O-tetradecanoylphorbol-13-acetate (TPA), ascorbic acid (AA), and others. PMA was used for the differentiation for the experiments as it is known to activate the NOX complex focused in the thesis.

2. AIMS OF THE THESIS

1. Review of literature on the topic of biomolecule oxidation.

2. To get acquainted with the preparation of samples, standardization, and use of spectroscopic methods.

3. Develop a brief overview of the reaction mechanism leading to biomolecule oxidation.

4. Evaluate the measured results and discuss them in relation to the literature.

3. LITERATURE REVIEW

3. 1 Monocytes and macrophages

3. 1. 1 Monocytes

Monocytes are heterogeneous cells that belong to the leukocyte family of immune cells. They are phagocytic cells and belong to the mononuclear phagocyte system. Before differentiation into macrophages, they flow in the organism's blood until they are needed at specific location in the body. They originate in bone marrow, similarly to other immune-type cells, such as lymphocytes or red blood cells.

The precursor of a monocyte is a promonocyte, a cell similar in structure to the monocyte, promonocyte is a derivation of a monoblast. These derivations take place inside the bone marrow in less than a day. When monocytes start circulating in the organism's blood, they are divided into two pools, a circulating pool and a marginating pool. The half-life of monocytes is quite organism-dependent, surging between 17 h and 71 h (van Furth & Beekhuizen, 1998). During their lifetime, they circle in the bloodstream and when required, they are activated, migrate into inflamed tissue, differentiate, and start an immune response (Benjamin *et al*., 2018). (Fig. 1)

Monocytes can be divided into groups based on CD14 and CD16 expression into three groups, classical monocytes, intermediate monocytes and nonclassical monocytes (Ziegler-Heitbrock *et al*., 2010). Classical monocytes have the ability to infiltrate tissues, produce inflammatory cytokines, and differentiate into inflammatory macrophages. Therefore, they are also called inflammatory monocytes (Jakubzick *et al*., 2017). Non-classical monocytes and intermediate monocytes can be found in the vasculature of patients with Deficits in Attention, Motor and Perceptual Abilities and differentiate into macrophages that are tissue resident or macrophages that fight against inflammatory responses to heal damaged tissue, anti-inflammatory macrophages (Mirjam & Broos, 2019).

Between 2% and 11% of monocytes are intermediate in their phenotype. These monocytes are very pro-inflammatory and participate in antigen presentation and ROS production, angiogenesis, and T-cell activation (de Souza *et al*., 2022). Classical monocytes range from 80% - 95%, and nonclassical monocytes are present between 2% and 8%.

3. 1. 2 Macrophages

Macrophages are immune cells derived from monocytes by differentiation. They are mononuclear phagocytes that circulate in the bloodstream. They belong to both adaptive and innate immunity (McKay & MacNaughton, 2012). In addition, unlike monocytes macrophages have a life span ranging from months to years inside a body (van Furth & Cohn, 1968). Whereas monocytes circulate in the bloodstream, monocytes remain inside different tissues and thus are named differently based on which tissue holds the macrophage. For example, Kupfer cells are macrophages inside the liver, microglial cells inside the brain, and osteoclasts are inside bones (Tao & Xu, 2016). When comparing the size of macrophages to the size of monocytes, the size of macrophages is generally reported to be larger (Lendeckel *et al*., 2022).

Macrophage activity can be promoted by cytokines excreted from T_H cells and other inflammatory factors; these activated macrophages are more powerful in pathogen elimination. In this elimination they phagocyte and secrete higher amounts of inflammatory factors, such as higher MHC class II molecules (major histocompatibility complex), which can be then presented back to T_H cells, the macrophage acting as APC (antigen presenting cell). This mutually benefits both cell types, macrophages acting not only as direct elimination, but also as a defence in becoming an APC (Tao & Xu, 2016).

From studies conducted previously, macrophages are divided into two types, M1 and M2 macrophages. These macrophage types differ mainly in their profile when associated with inflammation and are successive from the M1 type to the M2 type. M1 type macrophages are pro-inflammatory whereas M2 type macrophages are anti-inflammatory. The M1 macrophage phenotype is also against the regeneration process whereas the M2 phenotype is promotive to healing processes (Wang *et al*., 2019). It must be said however that this difference is hardly seen in *ex vivo* or *in vivo* human tissue analyses and experiments (Timperi & Ramos, 2022).

Even though the M1 M2 bimodal differentiation model is now widely used, it is also known that there is a large complexity between these models, thus revealing a spectrum of macrophage types (Mosser & Edwards, 2008; Xue *et al*., 2014). This spectrum was analysed when different stimuli were used, such as oleic acid, free fatty acids, high-density lipoproteins, or different combinations of other stimuli.

Macrophages are derived in two ways, differentiated from monocytes, thus being monocyte-derived macrophages, or originating from the embryonic phase and becoming part

of the tissue resident macrophages. Today, monocyte-derived macrophages are widely used in *in vitro* studies to deepen the knowledge regarding macrophages.

3. 1. 3 Monocyte differentiation

Monocytes are very versatile in the sense that they can differentiate into many cell types based on the need and the stimulus. These cells are then monocyte derived. Monocytes can differentiate into dendritic cells (DC) or macrophages (Italiani & Boraschi, 2014; Marzaioli *et al*., 2020). (Fig. 1)

There exist several stimuli which lead monocyte to differentiate to DC or macrophages and it has been discussed in the following sections.

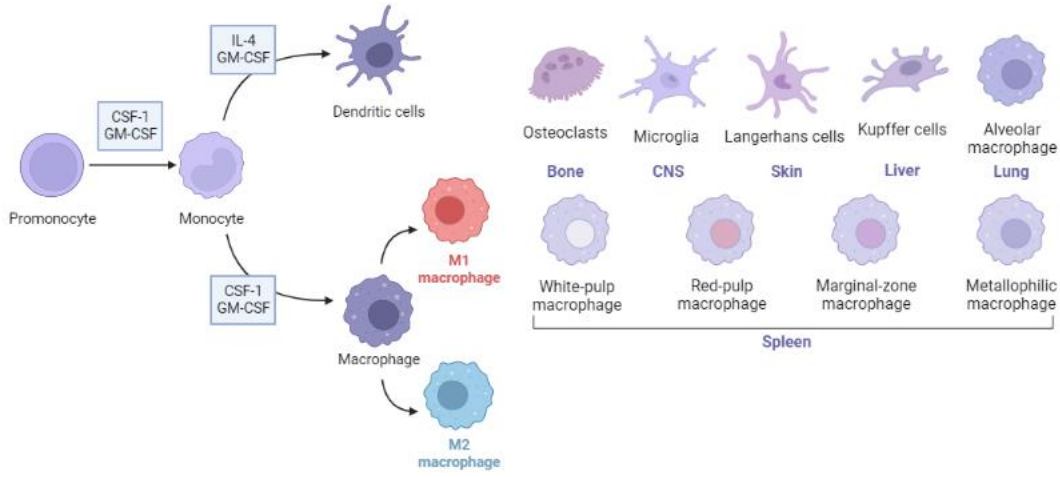

Figure 1: Scheme of differentiation from monocyte to macrophages or DC (left), Types of macrophages present in different body parts (right). [CNS- central nervous system, CSF-1- colony stimulating factor 1, GM-CSF- granulocyte-macrophage colony stimulating factor, IL-4- interleukin 4] Created in BioRender.com

3. 1. 4 Structure of macrophages

Macrophages are round-shaped mononuclear cells. However, the morphology of macrophages is dependent on their type and location inside the body. An example of this can be that adherent macrophages are more elongated and spindle-like with an amoeboid structure. They can also have a round shape that is dependent on their lamellipodial extensions (Paul *et al*., 2008; Tsai *et al*., 2011). Lee and co-workers also discovered that the morphology of a macrophage correlates with cytokine secretion and cellular activation (Lee *et al*., 2013).

An example of morphological differences between the M0, M1, and M2 types of macrophages is well seen in a study by Heinrich and co-workers who studied canine macrophages. The M0 type macrophages were found to be the smallest out of all the types, with

a small round shape, and with none or very little cytoplasmic extensions. The diameter of the cells was recorded at around 8 µm.

A portion of the M0 type macrophages had amoeboid morphology. This morphology is more observed in M1 type macrophages, however. The M1 type macrophages were mostly amoeboid in structure and had many fibrillary active processes, whose length ranged up to 5 µm. The overall diameter of the M1 type macrophages was approximately 15 µm. The M2 type macrophages were heterogeneous with 4 different morphologies ranging from amoeboid round shapes to spindeloid and bipolar structures measuring up to 35 µm (Heinrich *et al*., 2017).

3. 1. 5 Changes of expression during monocyte-macrophage differentiation

Changes of the expression of the cells during monocyte-macrophage differentiation were studied in recent years. The tables presented (Table 1-2) were adopted with modifications from a study that used the same differentiation agent as was used in this thesis.

Table 1: Ten most upregulated and downregulated genes in PMA-stimulated THP-1 macrophages compared with undifferentiated THP-1 monocytes. Adopted with a modification from Tuomisto *et al*., 2005

Gene
Upregulated
Interleukin-1 beta
Macrophage inflammatory protein 3, alpha
Matrix metalloproteinase-9
Fibronectin-1
Serina-threonine protein kinase 25
Disintegrin and metalloproteinase ADAM10
Regulator of G-protein signaling-7
Interleukin-2 receptor gamma
Monocyte differentiation antigen CD14
Cathepsin G
Downregulated
Interferon consensus sequence binding protein-1
Carbonic anhydrase II
Cote1 protein
Myb proto-oncogene protein
Butyrate response factor 2
Cyclin-dependent kinase 6 inhibitor Nidogen
Regulator of Fas-induced apoptosis
High mobility group protein 2
Sterol delta-7-reductase

Table 2: Twenty most upregulated proteins in PMA-stimulated THP-1 macrophages grouped into functional classes. Adopted with a modification from Tuomisto *et al*., 2005

Function	Protein
Intracellular signalling	Leukocyte antigen related protein phosphatase
	A-kinase anchor protein 149
	Rabaptin-5
	RanBP1
	NM23-H1 (nucleoside Di-P Kinase)
Cell division/growth	Signal-induced proliferation-associated gene
	Cyclin-dependent kinase-1
	Cell division cycle 27
	CLIP-115
	Proliferation antigen Ki-67
Transcription and translation	Rnase HI
	TFII-I
Cell adhesion	Kalinin B1
	CD36
Inflammation	Cyclooxygenase-2 (COX-2/PGHS)
Oxidative stress	p47phox
Cell death factors	Caspase-1
	Caspase-6
	Caspase-8
	TRADD

Legend: TRADD- TNFR1-associated death domain protein

The studies that were conducted on patients show similar results. The expression of genes during monocyte-macrophage differentiation was regulated differently and thus can be used as a signal for patients developing or prone to developing atherosclerosis or other diseases (Korman *et al*., 2014). It was also discovered that the changes during the differentiation are quite significant in the lipid-related transcriptome, such as PUFA (polyunsaturated fatty acid) (Wallner *et al*., 2014).

3. 2 NADPH oxidase and its function

NADPH oxidase (NOX) is a oxidise complex present on membranes of cells. It was first discovered in phagocytic cells. The term NOX specifically refers to the transmembrane portion of the protein ($gp91^{phox}$), though nowadays the term is equivalent to the entire enzyme complex (DeCoursey *et al*., 2001). This phagocytic NOX, the $gp91^{phox}$ protein, is now further identified as NOX2.

The molecular weight of NOX2 was assigned to be 91 kDa by western blot analyses (Harper *et al*., 1985). The subunits of the complex were further identified and named as $p47^{phox}$ (phox phagocytic NADPH oxidase), an organising complex, $p67^{phox}$, which activates one of GTP-binding (guanosine triphosphate-binding) proteins Rac1 and Rac2, each of them present in different cell types, and $p40^{phox}$, which is a cytosolic factor (Abo *et al*., 1991; Knaus *et al*., 1991; Nunoi *et al*., 1988; Volpp *et al*., 1988; Wientjes *et al*., 1993). These subunits when combined create an activated NOX2. (Fig. 2)

3. 2. 1 Subunits of NADPH oxidase

The structure of NOX2 consists of 6 helixes that go through the membrane, intracellular and extracellular loops with 2 b-type heme groups and a cytosolic domain with $FADH_2$ (flavine adenine dinucleotide) and NADPH-binding domains. The NOX2 is coupled to $p22^{phox}$, that when activated binds further to p47 through a pattern recognition receptor domain. It was not yet clearly identified how many transmembrane segments of $p22^{phox}$ are present; it is however, by experiments and hypothesises highly theorised, that there are two or four helixes of $p22^{phox}$ (Dahan *et al*., 2002; Rae *et al*., 2000; Taylor *et al*., 2004; Vermot *et al*., 2021). These two membrane subunits compose flavocytochrome b558. The flavocytochrome b558 then acts as the catalytic core of the enzymatic complex and associates with the other subunits, $p47^{phox}$, $p67^{phox}$, and $p40^{phox}$ along with the small GTPase Rac. The subunits are present in cytosol when not needed and after stimulation, they translocate to the catalytic core and bind to it (Gardiner *et al*., 2013). (Fig. 2)

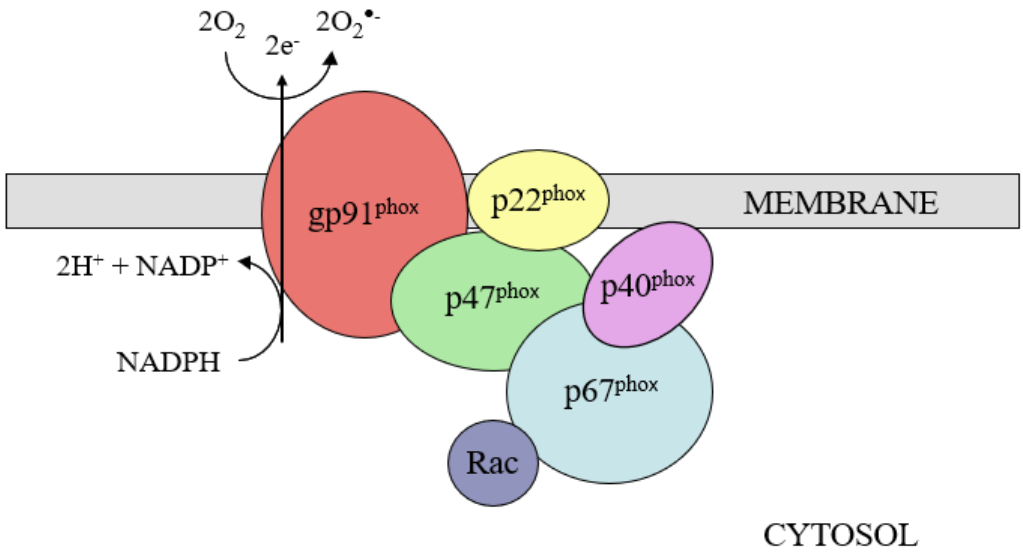

Figure 2: Structure of NADPH oxidase, namely the NOX2 isoform. Adopted with modification from Gardiner *et al*., 2013

3. 2. 2 Members of the NADPH oxidase enzyme family

After the discovery of NOX2 (Hattori, 1961.; Segal & Jones, 1978; Segal & Jones, 1979), analogous enzyme systems in other cell types, such as fibroblasts, vascular tissue cells, or tumour cells, were reported (Arbault *et al*., 1997; Dahan *et al*., 2002; Griendling *et al*., 2000). Researchers reported a NOX2 analogue NOX1 (Bánfi *et al*., 2000; Kikuchi *et al*., 2000; Suh *et al*., 1999), which then led to discoveries of the other analogues, NOX3, NOX4 and NOX5 (Bánfi *et al*., 2001; Geiszt *et al*., 2000; Kikuchi *et al*., 2000) and dual NADPH oxidases DOUX1 and DOUX2 (De Deken *et al*., 2000; Dupuy *et al*., 1999).

The NOX2 present in the complex is exclusively a part of the electron transfer processes, the $p22^{phox}$ subunit stabilising the unit. This subunit is however required in other NOX complexes, namely NOX1, NOX3 and NOX4 to form a heterodimer with them (Bedard & Krause, 2007). The phox proteins are multidomained, forming interactions with each other via their domains. Because NOX2 is the best-known member of the NOX family, most of the NOX enzymes capabilities are described on the NOX2 enzyme complex.

The different members of the NOX enzyme family differ from each other in term of localization inside an organism, in which they are active, and in their sequence. They also require different cytosolic factors. For example, NOX1 and NOX3 need cytosolic factors which are homologous to the subunits of NOX2 (refer to Fig. 3 for details).

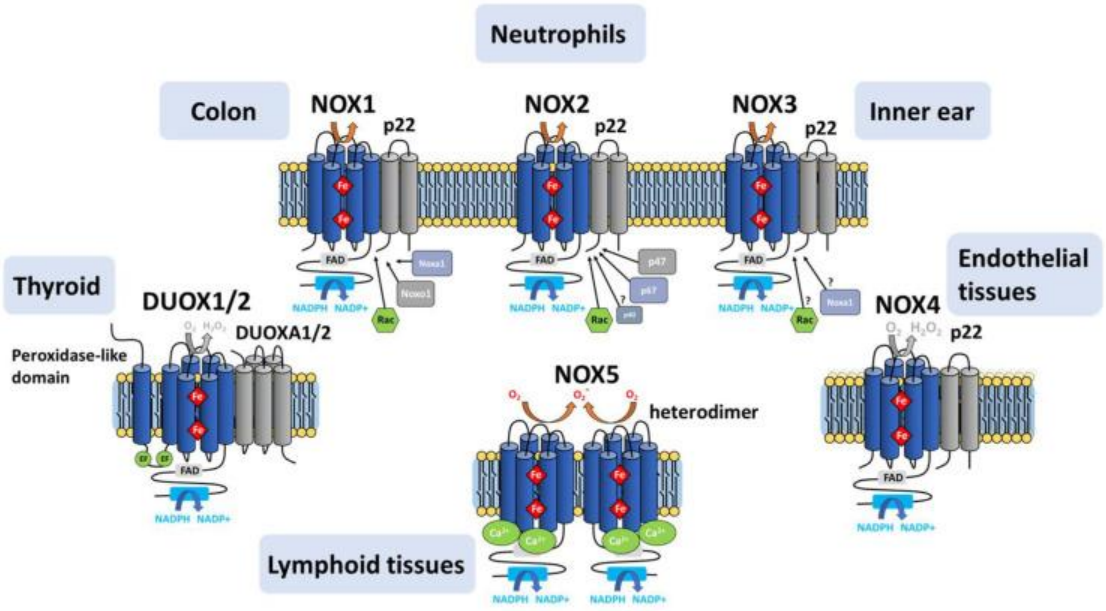

Figure 3: Representation of the NADPH oxidase isoforms. Adopted with modification from Vermot *et al*., 2021

Even though the enzyme isoforms have similar structure and their functions are alike, the activation that occurs in them is varied. Essential subunits for NOX1 activity are $p22^{phox}$, NOXO1 (NADPH oxidase organiser 1), NOXA1 (NADPH oxidase activator 1) and the GTPase Rac. Subunits needed in NOX2 activation are $p22^{phox}$, $p47^{phox}$, $p67^{phox}$ and Rac. For the NOX3 to be in an activated form, it demands $p22^{phox}$ and NOXO1 and depending on the species requires NOXA1, Rac can participate in NOX3 activity, but it is not necessary when compared with the other subunits. The only constantly active out of the family NOX4 requires $p22^{phox}$ *in vivo*. In the activation of NOX5, DUOX1 and DUOX2, Ca^{2+} ions must be present. For DUOX1 and DUOX2 to function properly, they need to be associated with the maturation factors DUOXA1/DUOXA2 (Dual NADPH oxidase activator). NOX1, 2, 3 and 5 produce mainly $O_2^{\bullet-}$, NOX4 produces mainly H_2O_2, and DUOX1 and DUOX2 produce both $O_2^{\bullet-}$ and H_2O_2 (Vermot *et al*., 2021).

When it comes to NOXs present in macrophages, there were 4 out of the 7 NOXs reported as expressed in phagocytes (Moghadam *et al*., 2021). Specifically, NOX2 was discovered as the first NOX and isolated primarily from phagocytes, NOX1 was discovered in contributing to liposaccharide-derived ROS (Maitra *et al*., 2009), NOX4 and NOX5 were also discovered to be present in macrophages.

3. 2. 2. 1 NADPH oxidase 4

Compared to other NOXs, NOX4 is a consistently active enzymatic complex highly expressed in fibroblasts, osteoclasts, endothelial cells, and kidneys. Its maturation depends on $p22^{phox}$, just as NOX2 maturation but is not in need of activation. This particular complex produces mainly H_2O_2, even in the absence of SOD (superoxide dismutase) (Nisimoto *et al*., 2014). It is also a source of $O_2^{\bullet-}$ in some pathophysiological environments (Kuroda *et al*., 2010). As a main source of ROS, NOX4 is responsible for cell proliferation, apoptosis, angiogenesis, and others (Vermot *et al*., 2021). In recent years, NOX4 has also been found to be beneficial in vascular cells by protecting the vasculature when it is exposed to stress (Schröder *et al*., 2012). It has also been suggested that H_2O_2 produced by NOX4 leads to NOX2 activation (Chen *et al*., 2014; Evangelista *et al*., 2012; Kim *et al*., 2017).

3. 2. 3 Assembly of NADPH oxidase in cells

Before NOX is activated, some activators can prime the enzyme, and once primed, it can lead to a greater and faster response to the pathogen response. Some activators consist of PAF^5(platelet-activating factor), TNFα (tumour necrosis factor) or fMLF (formyl-methionyl-leucyl-phenylalanine) (Vermot *et al*., 2021). Priming can, however, cause oxidative damage to tissues surrounding activated cells (Parvez *et al*., 2018).

For NOX to become active, several steps are desired. In its inactive state, the enzyme complex is without several of its domains. NOX2 activation is initiated by several upstream events at the cellular level. When tissue-resident macrophages recognize pathogens in the system, they activate proinflammatory chemoattractant mediators (Nguyen *et al*., 2017). Later on, neutrophils migrate from the vasculature to the pathogen location. The pathogen is then countered by various methods, counting macrophage mannose receptors and scavenger receptors, microorganism-specific motifs, direct interaction, through opsins or intermediatory adaptor biomolecules that improve the pathogen's recognition (DeLeo *et al*., 1999; Yang *et al*., 2012). When recognised, the phagocyte begins to activate NOX2 by phosphorylating other subunits, mainly $p47^{phox}$, mobilizing cytosolic partners of the NOX2 complex (Fig. 4). The subunits are translocated to the flavocytochrome b558 and the catalytic reaction of $O_2^{\bullet-}$ production begins. Rac-GDP present in cytosol is then also transferred to the membrane and when exchanged for GTP, binds $p67^{phox}$ to the rest of the enzyme, activating the NOX2. When enough effectors that kill the pathogen are released, the cascade ceases.

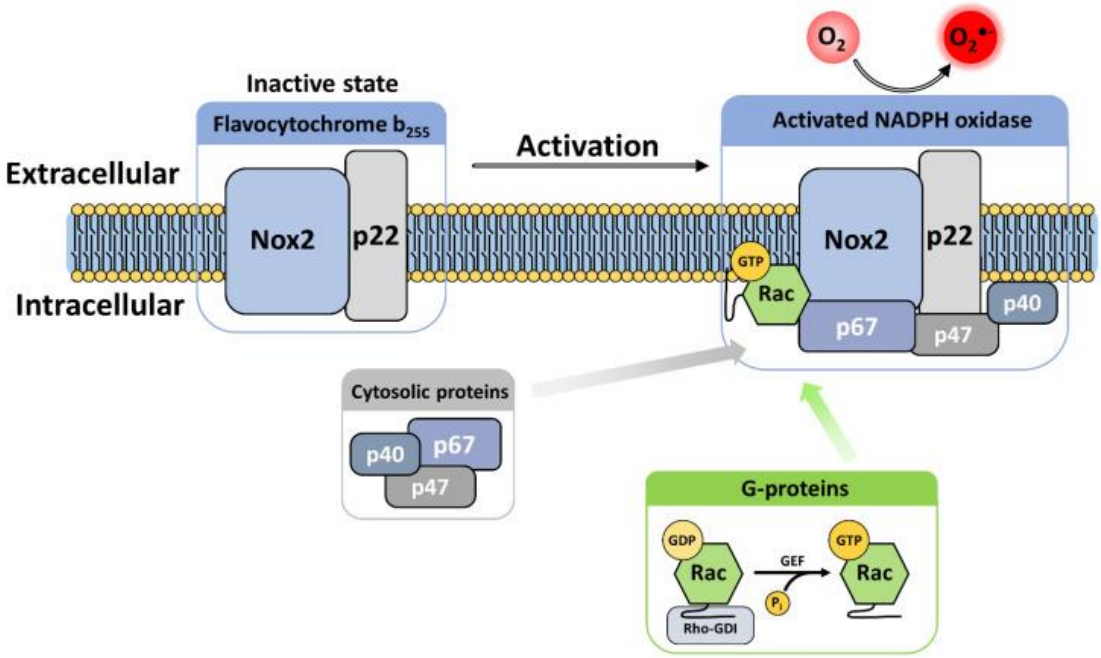

Figure 4: Activation process of the phagocytic NADPH oxidase, namely its NOX2 isoform. Adopted with modification from Vermot *et al*., 2021

3. 2. 4 Mechanism of NADPH oxidase

The family of NOXs are ROS-generating enzymes. Because different NOXs are present in different parts of the organism, the function of each NOX is reported to be different. These functions are simplified in Table 3.

Table 3: Purpose and activation of NADPH oxidases in stem cells and cancer stem cells. Adopted with modification from Skonieczna *et al*., 2017

Process	Expression/activity of NOX	Effects/mechanism	Reference
Differentiation	↑ NOX2	Differentiation of stem cell/ROS-dependent Notch signalling pathway	Kang *et al*., 2016
	↓ NOX4	Myogenesis, C2C12 differentiation/ ERK1/2 phosphorylation, MAP kinases	Acharya *et al*., 2013
	↑ NOX2 ↑ NOX4	CPCs → ↑ c-kits (+) cells/unknown mechanism	Nadworny *et al*., 2013
	↑ NOX4	Differentiation of endothelial cells into smooth muscle cells/TGFβ-1-dependent NOX4/H_2O_2 upregulation NOX4/H_2O_2 dependent	Xiao *et al*., 2009

Table 3: Continued

Process	Expression/activity of NOX	Effects/mechanism	Reference
Differentiation	↑ NOX4	(i) NCSCs differentiation to neural cells	Lee *et al*., 2014; Mandal *et al*., 2011; Simone *et al*., 2012
		(ii) 2T3 preosteoblast differentiation	
		(iii) Renal progenitor cells differentiation to profibrotic cells	
	↓ NOX4	NCSCs death or retarded growth of PNS	Lee *et al*., 2014
Stem cell self-renewal	↑ NOX4	Proliferation of neural stem cells/superoxide dependent	Topchiy *et al*., 2013
	↑ NOX3	↑ Proliferation of mouse spermatogonial stem cells/unknown mechanism	Morimoto *et al*., 2015
	↓ NOX4	↓ Proliferation and migration of ADSCs/ ↓ ERK1/2, Akt, ↓ PDGFβ1	Kim *et al*., 2012
	↓ NOX	Proliferation of mesenchymal stem cells/ Nanog/Oct4 (TFs)	Sun *et al*., 2015
	NOX2 NOX4	↑ Senescence of Ang. II-stimulated endothelial cells/unknown mechanism	Li *et al*., 2011
Cancer stem cell growth and survival	NOX2	↑ Proliferation of pancreatic cancer cells (SW 1990 and BxPC-3)/ NF-κB/STAT3 activation	Zhang *et al*., 2016
	↑ NOX1	↑ Enrichment of breast cancer stem-like cell population/ RAS/Erk1/2/NOX1 activation	Pluchino & Wang, 2014
	↓ NOX2, NOX4, NOX5	↑ Survival of prostate stem-like cells	Shimada *et al*., 2013
Cancer stem cell drug resistance	↑ NOX2	↑ Resistance of patient-derived glioblastoma stem cells and chronic myeloid leukaemia stem cells to tyrosine kinase inhibitors/NOX2/Erg1/Fyn upregulation	Irwin *et al*., 2015

Legend: ADSC- adipose derived stem cell, CPC- cardiac precursor cell, MAP- mitogen activated protein, NCSC- Neutral crest stem cell, TF- transcriptional factor, PNS- peripheral nervous system

3. 2. 5 Occurrence of NADPH oxidase in cell

Depending on the cell type, the enzyme complex on cell membranes, including internal membranes like membranes of a nucleus or endoplasmic reticulum (ER) and mitochondria

are different (Ago *et al*., 2010; Ambasta *et al*., 2004; Kuroda *et al*., 2005). Recent studies also confirmed that the enzyme originated in prokaryotic cells when they reported prokaryotic homologs of the NOX complex (Hajjar *et al*., 2017).

The isoforms present in ER are NOX2 and NOX4, as regulators of blood pressure and are also involved in hypertension (Li *et al*., 2010; Young *et al*., 2012). The NOX4 generated H_2O_2 could also promote protein folding (Santos *et al*., 2014). Endoplasmic reticulum related stress is known to be related to increased NOX4 expression. If there exists a pharmacological drug against ER-bound NOX4, it could prevent ER-developed hypertension (Wenceslau *et al*., 2018). There is also speculation of NOX1 being present in ER, however it can only be an immature version of the enzyme (Laurindo *et al*., 2014).

In mitochondria there was NOX4 reported in many cell types (Dikalov, 2011; Peng *et al*., 2023). Since mitochondria is a key ROS producer, it can stimulate NOX in other parts of the cell. In monocyte-derived DC, NOX5 is also present in mitochondria (Marzaioli *et al*., 2017). The localization of NOX based on cell type and tissue is summarized and presented in Table 4

Table 4: Expression of NOX family members and their components in various tissues or cells. Adopted with modification from Panday *et al*., 2014

NOX type/component		Expression observed in		References
		Tissue	Cells	
NOX isoforms				
1	NOX1	Colon and vascular smooth muscle, prostate, uterus	Endothelial cells	Bedard & Krause, 2007
		Colon epithelia	Osteoclasts	Bedard & Krause, 2007; Kamdar *et al*., 2013
		Uterus and placenta	Retinal phagocytes, neurons, astrocytes and microglia	Bohle *et al*., 1977; Fukata *et al*., 2009
		Rectum		Wada *et al*., 2000
2	NOX2 ($gp91^{phox}$)		Phagocytes/granulocytes-induced through bacterial LPS	Snelgrove *et al*., 2004
			Human umbilical vein endothelial cells	Snelgrove *et al*., 2006
			Coronary microvascular endothelial cells	Suliman *et al*., 2001

Table 4: Continued 1

NOX type/component		Expression observed in Tissue	Cells	References
NOX isoforms				
2	NOX2 ($gp91^{phox}$)		Cardiomyocytes	Martin *et al*., 2002
			CNS, endothelium, VSMCs, fibroblasts, skeletal muscle, hepatocytes and hematopoietic stem cells	Lin *et al*., 2009
3	NOX3	Foetal kidney		Bedard & Krause, 2007
		Liver, lung and spleen, Low levels in the adult colon and kidney		Chakraborti *et al*., 2013
		Inner ear		Kawai & Akira, 2007
4	NOX4	Kidney	Mesangial cells	Kamdar *et al*., 2013; Nada *et al*., 2012
		Liver	Smooth muscle cells	Bedard & Krause, 2007; Park & Lee, 2013
		Ovary and eye	Fibroblasts	Heyworth *et al*., 1991; Noguera *et al*., 2001
			Keratinocytes	Lin *et al*., 2009
			Osteoclasts	Hoff & Buttgereit, 2014; Lin *et al*., 2009
			Endothelial cells	Babior, 1999
			Neurons	Gao *et al*., 2012
			Hepatocytes	Bureau *et al*., 2001
5	NOX5	Spleen, testis, mammary glands and cerebrum	VSMCs	Bedard & Krause, 2007; Theivanthiran *et al*., 2012
		Foetal brain heart, kidney, liver, lung, skeletal muscle, spleen, thymus		Fink, 2003
		Prostate		Akaike, 2001
		Lymphatic tissue, endothelial cells		Batra *et al*., 2012
6	DUOX1	Thyroid, cerebellum and lungs	Thyroid cells	Bedard & Krause, 2007

Table 4: Continued 2

NOX type/component		Expression observed in Tissue	Cells	References
NOX isoforms				
6	DUOX1	Illeum, cecum, and floating colon		Kawahara *et al*., 2004
		Respiratory tract epithelium		Harper *et al*., 2005
7	DUOX2	Colon pancreatic islets and prostate	Thyroid cells in primary culture	De Deken *et al*., 2000; Edens *et al*., 2001
		Stomach, duodenum, ileum, jejunum, cecum, sigmoidal colon, floating colon and rectum		El Hassani *et al*., 2005
		Pancreas		Wu *et al*., 2011
		Tracheal and bronchial epithelium		Harper *et al*., 2006
		Thyroid		Yoshizawa-Ogasawara *et al*., 2013
Components of NOX				
1	p67phox	Kidney	Neutrophil	Feng *et al*., 2012; Nunoi *et al*., 1988; Volpp *et al.,* 1988
2	p47phox		Neutrophils	Clark *et al*., 1990
3	p40phox		Mononuclear cells	Wientjes *et al*., 1993
4	p22 phox	Human coronary arteries		Azumi *et al*., 1999
5	Rac1		Neutrophils	Abo *et al*., 1991
6	Rac2		Hematopoietic cells	Gu *et al*., 2003
7	NOXO1, NOXA1	Colon		Bedard & Krause, 2007

Legend: CNS- central nervous system, LPS- liposaccharides, VSMC- Vascular smooth muscle cell

3. 2. 6 Superoxide anion radical formation by NADPH oxidase

The main role of NOX is to form $O_2^{\bullet-}$ as a product of a reaction. The NOX subunit catalyses the transfer of electrons through the membrane and $O_2^{\bullet-}$ is formed based on the reaction scheme mentioned (I) (Babior, 1999).

$$2\ O_2 + NADPH \rightarrow 2\ O_2^{\bullet-} + NADP^+ + H^+ \quad (I)$$

$O2^{\bullet-}$ is then dismutated by SOD or spontaneously to H_2O_2 (II-III) (Sharma *et al*., 2012). It was discovered that NOX could be the main source of $O2^{\bullet-}$ production (Sahoo *et al*., 2016).

$$2\ O_2^{\bullet-} + 2\ H^+ \rightarrow H_2O_2 + O_2 \quad \text{(II)}$$

$$2\ O_2^{\bullet-} + 2\ H^+ \xrightarrow{SOD} H_2O_2 + O_2 \quad \text{(III)}$$

Through these reactions, a cascade of other reactions occurs, mainly the Fenton's and Haber-Weiss reactions (Fig. 5).

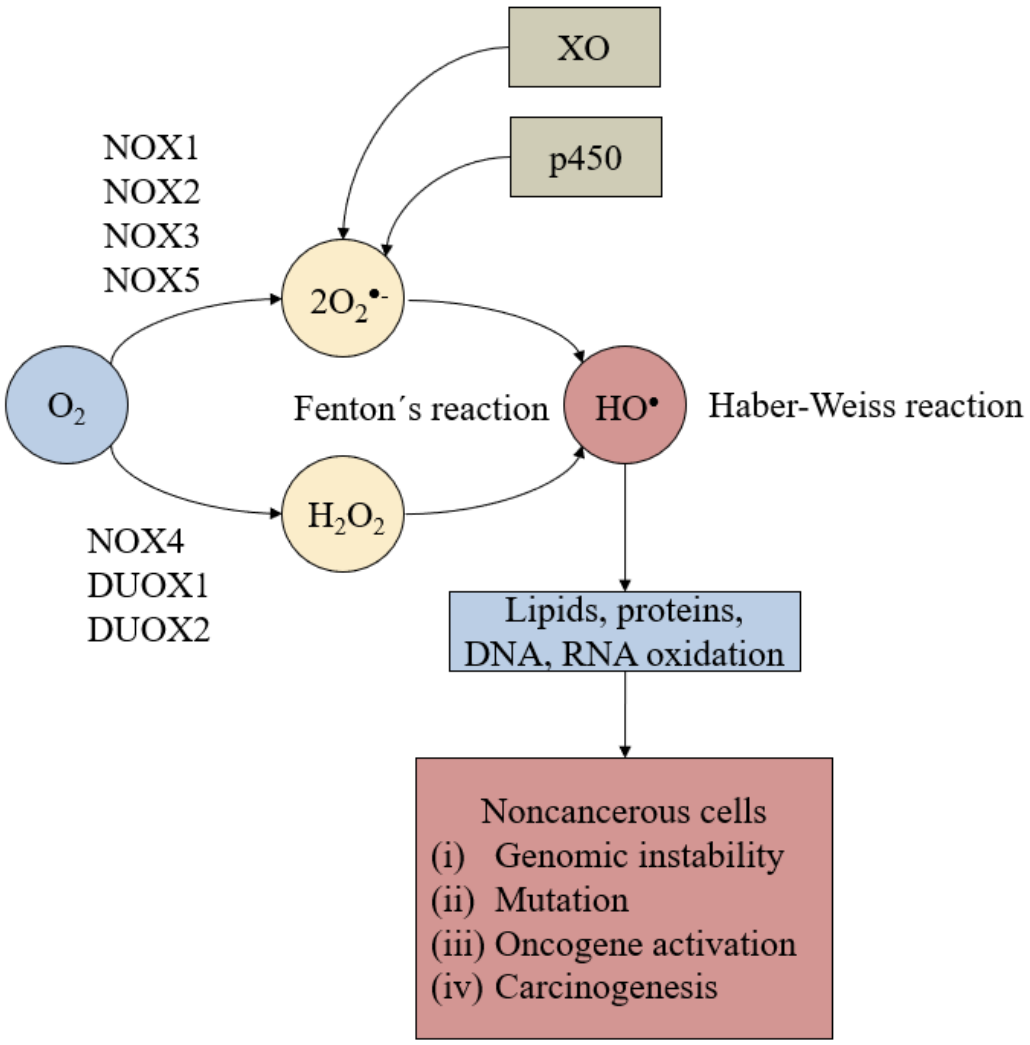

Figure 5: Intracellular factors and consequences of ROS overproduction. Overproduction of $O_2^{\bullet-}$ and H_2O_2 by NOX (NOX and DUOX), cytochrome c oxidase, or xanthine oxidase (XO). Adopted with modification from Skonieczna *et al*., 2017.

3. 2. 6. 1 Fenton's reagent/ Haber Weiss reaction

The Fenton's/Haber Weiss reaction describes a series of reactions that can lead to the formation of OH^-, and the end catalytically decomposes H_2O_2 by Fe^{2+}. The series of reactions was described in the first half of the 20th century (Barb *et al*., 1951; Haber & Willstätter, 1931; Haber *et al*., 1934).. The Fenton's reaction is a reaction of H_2O_2 with Fe^{2+}. For the entire chain of reaction to happen, there must be catalytic metals, like Fe or Cu, present. The Fenton's and Haber-Weiss reactions are presented in equations (IV-VI), which were adopted and modified from (Shad *et al*., 2023). These equations represent the decomposition of H_2O_2. The Haber-Weiss reaction does not probably have biological significance in the cytoplasm, but in extracellular fluids, atherogenesis can have some value (Liochev & Fridovich, 2002). The series of equations is of significance in oxidative damage in degenerative diseases (Das *et al*., 2015).

$$Fe^{2+} + H_2O_2 \rightarrow Fe^{3+} + HO^{\bullet} + HO^- \text{ (IV)}$$

$$HO^{\bullet} + H_2O_2 \rightarrow O_2^- + H^+ + H_2O \text{ (V)}$$

$$O_2^{\bullet-} + H_2O_2 \xrightarrow{Fe^{3+}/Fe^{2+}} HO^{\bullet} + HO^- + O_2 \text{ (VI)}$$

The chain length of the process described in the equations above is limited by the chain termination steps occurring in cells. These terminations are described in Equations below (VII-X) (Liochev & Fridovich, 2002). The terminations can be achieved by various antioxidants and enzymes, that have the role of protecting the cell against ROS and other dangerous substances.

$$O_2^{-} + O_2^{-} + 2\,H^+ \rightarrow O_2 + H_2O_2 \text{ (VII)}$$

$$O_2^{-} + HO^{\bullet} \rightarrow O_2 + HO^- \text{ (VIII)}$$

$$HO^{\bullet} + HO^{\bullet} \rightarrow H_2O_2 \text{ (IX)}$$

$$HO^{\bullet} + Fe^{2+} \rightarrow HO^- + Fe^{3+} \text{ (X)}$$

Reactive oxygen species produced by these reactions also cause damage through lipid peroxidation and other oxidative damage processes (Das *et al*., 2015).

3. 3 Biomolecule oxidation

3. 3. 1 Reactive oxygen species

Reactive oxygen species is a generic term for a large family of oxidants derived from molecular oxygen (Sies *et al*., 2022). They are part of a larger group of reactive species (RS), such as reactive halogen, electrophile, nitrogen, selenium, or sulphur. The RS undergo reduction-oxidation reactions and forms oxidative modifications of the biomolecules as a by-product. They are also an important part of biomolecule oxidation.

Formation of ROS usually consists of successive reductions of molecular oxygen O_2, some of these formations are $O_2^{\bullet-}$, H_2O_2, $HO^{\bullet}$ among others (Sharma *et al*., 2012) (Fig. 5). Some of these molecules have specific functions in the cell and are formed during different reactions. There are two groups into which ROS are divided, based on how many electrons are present in radical (one electron, unpaired electrons) and non-radical (two electrons, no unpaired electrons) (Li *et al*., 2016) (Table 5)

Table 5: Division of reactive oxygen species and some of their most common molecules

Radical		Non-radical	
Superoxide anion radical	$O_2^{\bullet-}$	Hydrogen peroxide	H_2O_2
Hydroxyl radical	$HO^{\bullet}$	Ozone	O_3
Peroxyl radical	$RO_2^{\bullet}$	Hypochlorous acid	$HOCl^-$
Hydroperoxyl radical	$HO_2^{\bullet}$	Organic hydroperoxide	ROOH
Alkoxyl radical	$RO^{\bullet}$	Peroxynitrite	NO_3^-
Nitric oxide	$NO^{\bullet}$		

Reactive oxygen species can be formed in many parts of the cell compartments-mitochondria, peroxisomes, and ER are the main sources (Hansen *et al*., 2006; Lambert & Brand, 2009). The formation is well reported in the mitochondrial electron transport chain, an aerobic process that supplies energy in the form of NADPH and $FADH_2$ (Schieber & Chandel, 2014). It is also present in metal-catalysed oxidation (Cheignon *et al*., 2016).

Because ROS are formed regularly inside the cell and can cause damage, cells have created an antioxidant system, which protects them. These antioxidant defence systems are very important because without them, levels of ROS become too high to deal with. This damage can lead to tumorigenesis promotion and many other unwanted processes within the cell/organ system (Neumann *et al*., 2003).

3. 3. 2 Lipid peroxidation

Lipid oxidation, known also as lipid peroxidation, occurs between fatty acid chains and ROS, resulting in lipid degradation, otherwise known as rancidity (Mozuraityte *et al*., 2016). It has also been linked to several diseases, such as Alzheimer´s. It also plays a role in various processes, such as atherogenesis (Marín-García, 2007).

One of the most common places for ROS to react is with exposed lipids of the cell membrane. As PUFAs are highly present in the cell membrane, lipid peroxidation occurs often (Mao *et al*., 2022).

Lipid peroxidation as a process can be divided into three distinct processes, initiation, propagation, and termination.

Initiation (reaction XI) is commonly caused by an abstraction of a hydrogen atom by an RS ($X^{\bullet}$) with a methylene group (RH) (Halliwell & Gutteridge, 2015). From this reaction a non-reactive species (XH) and carbon radical ($R^{\bullet}$) is formed. The reaction weakens the bond energy of C-H bonds of adjacent carbon atoms when double bonds are present, even more so if the double bond is on both sides of the C-H bond. This means that the more double bonds are present in the PUFA, the more prone to oxidation it is. Radiation-induced peroxidation is also possible; however, it is inhibited to some extent by $HO^{\bullet}$ scavengers. When compared to $HO^{\bullet}$, $NO^{\bullet}$ and $O_2^{\bullet-}$ are not reactive enough to abstract $H^{\bullet}$ from lipids to initiate the peroxidation. $HO_2^{\bullet}$ on the other hand is reactive enough to abstract the $H^{\bullet}$ from some PUFAs for example, linoleic acid or linolenic acid can be presented. Despite the ability to initiate the peroxidation, $HO_2^{\bullet}$ was not yet discovered as an initiator of lipid peroxidation *in vivo* (Halliwell & Gutteridge, 2015).

$$X^{\bullet} + RH \rightarrow R^{\bullet} + XH \text{ (XI)}$$

In the propagation stage (XII) new carbon radicals are formed, which react with O_2 to form new carbon radicals. The carbon radical formed in the previous stage stabilises itself by rearranging its molecule and forming a conjugated diene. The carbon radical formed during initiation is combined with O_2 and forms a peroxyl radical. The less likely reaction cross-links two fatty-acid chains together (Halliwell & Gutteridge, 2015).

$$R^{\bullet} + O_2 \rightarrow RO_2^{\bullet} \text{ (XII)}$$

In the termination stage (XIII), the formed radical reacts with the original substrate and forms an organic hydroperoxide and one new radical (Cai, 2005). If singlet oxygen ($^1O_2$) is present, the termination stage removes two peroxyl radicals. This can cause chemiluminescence, which sometimes occurs during peroxidation and can be detected (Halliwell & Gutteridge, 2015).

$$RO_2^{\bullet} + RH \rightarrow ROOH + R^{\bullet} \text{ (XIII)}$$

When the substrate has depleted, the radicals form bonds between themselves, thus becoming non-radical, and finally terminating the chain reaction (Cai, 2005).

3. 3. 3 Protein oxidation

Proteins can be modified by oxidation. This oxidation may be either reversible or irreversible, changing the protein indefinitely. Some protein oxidations, mainly reversible ones, are thought to be relevant in certain cellular processes. The irreversible protein oxidations are mostly seen as damaging, contributing to diseases and damage on a cellular level (Møller *et al*., 2011). As an example, irreversible protein oxidations highly occur in patients with degenerative diseases like cystic fibrosis or Alzheimer´s disease (Halliwell & Gutteridge, 2015).

Oxidation can occur in a direct or indirect way, oxidising the protein by itself or with a mediator. The reactivity and mechanism of production also varies based on which ROS was the one behind the oxidation. Proteins have various markers, which signify how much of the proteins was oxidised (Therond, 2006).

The most well known oxidations are carbonylations, lipoxidations, glycosylations, nitration/nitrosylations, oxidations of sulphur and aromatic moieties (Kehm *et al*., 2021).

3. 3. 4 Nucleic acid oxidation

Nucleic acids are highly researched because of their impact on pathogenesis and other non-wanted outcomes, such as diseases. Some oxidative damage is necessary for an organism, but only in some capacity. Therefore, this stress is called ‘eustress’ (Sies *et al*., 2017). Whereas in proteins or lipids, the molecules that have been caused damage can be replaced, nucleic acid must be repaired for the organism to function properly (Chao *et al*., 2021).

3. 4 Products during biomolecule oxidation-endoperoxides and ketones

3. 4. 1 Malondialdehyde

Malondialdehyde (MDA), sometimes called malonaldehyde is one of the final products of lipid peroxidation that is generated, more specifically it is generated as a product of PUFA peroxidation. Next to 4-Hydroxy-2-trans-nonenal (HNE) it is the most common marker for lipid peroxidation.

Several hypothesises have been proposed as the main origin of MDA in *in vivo* conditions. One of them is based on the fact, that the MDA precursor is non-volatile. The process of this MDA formation resembles prostaglandin formation (Pryor & Stanley, 1975). This hypothesis was later confirmed when MDA as a decomposition product was formed during lipid oxidation (Frankel & Neff, 1983). Another two hypotheses took MDA formation as a product of successive hyperoxide formation and β-cleavage of fatty acid chains (Esterbauer *et al*., 1991). Also, there is a reported generation of MDA from prostaglandins (Hecker & Ullrich, 1989). Due to its ability to form Michael adducts with thiol groups, cross-link, and cause mutagenesis, MDA is considered toxic (Esterbauer *et al*., 1991). It can also form bonds with functional groups of DNA, RNA, proteins or lipoproteins (Esterbauer & Cheeseman, 1990). The amount of MDA highly increases in cells, that are experiencing oxidative stress, and therefore from ROS. Whether or not to classify MDA as a toxic chemical, there had been discussion (Del Rio *et al*., 2005). Its toxicity however is not more severe than HNE, isoketals or levuglandins (Halliwell & Gutteridge, 2015). It has been reported that MDA is metabolised in mammalian tissue. Aldehyde dehydrogenases oxidise the MDA to malonic semialdehyde, which then decarboxylates to acetaldehyde (Halliwell & Gutteridge, 2015). MDA is often used as a marker of oxidative stress because of its increased formation as a result of ROS production.

3. 5 Detection methods

3. 5. 1 U-937 cell line and cell viability assays

The U-937 cell line was isolated in 1976 in the United States from a male human patient diagnosed with generalised lymphoma and therefore is considered a myeloid leukaemia cell line, more specifically, a promonocytic human myeloid leukaemia cell line (Sundström & Nilsson, 1976). The U-937 cell line is used primarily in conjunction with the THP-1 cell line for research on monocytic mechanisms and behaviour, and as the cells are uniform and unlimited, research with these cell lines is appropriate. It was also discovered that the U-937 cell line carries the t(10;11)(p13;q14) translocation, which creates a fusion of the

MLLT10 gene and the PICALM assembly protein. This fusion is important for the tumorigenicity of the cell line (Strefford *et al*., 2001) and thus serve as a good model system (Chanput *et al*., 2015).

A great advantage of using the U-937 cell line is the fact that the cell line does not have a Hayflick limit, which means that its telomerase is functioning indefinitely, while in other cell lines after 50 mitoses, cells go through apoptosis (Golubev *et al*., 2003; Hayflick & Moorhead, 1961; Nalobin *et al*., 2018; Zvereva *et al*., 2010).

The U-937 cell line is used more frequently due to its higher maturation stage because of its tissue origin.

Trypan blue is a chemical commonly used for viability assays, as it's very simple and quick. This test is based on the principle that trypan blue stain only stains already dead cells, thus distinguishing alive cells from the dead ones.

MTT assay is widely used for cytotoxicity assays as well as viability tests. It is based on the chemical reduction that happens inside cells that reduces MTT, which appears yellow to purple formazan. This reaction measures the metabolic activity of the cells.

3. 5. 1. 1 Cell differentiation

The U-937 cell line is used to study cell differentiation directed toward macrophages or promonocytes after exposing the cells to inducers/chemicals. Depending on the aim of the study, different agents for differentiation have been used in studies. The most frequently used chemicals for differentiation are retinoic acids, TPA (Chun *et al*., 2001), 1,25-dihydroxy vitamin D3 (VD3) (Rots *et al*., 1999) or AA. However, the most used chemical for differentiation is PMA.

After U-937 cells are exposed to the chosen chemical compound, the differentiation process starts caused by abiotic stress due to the chemical. The process takes ideally 48 to 72 h for the cells to fully differentiate into the macrophage-like morphology. During this differentiation process, ROS are known to be formed.

The properties of the differentiated U-937 cells are not well known. Cells treated with PMA show higher CD11b, an integrin molecule on the surface of leukocytes, and PKC (protein kinase C). This mimics PKC activator diacylglycerol (Yamamoto *et al*., 2008). A different property is the ability of the cell line to start adhering because of PKC, which results in AP1 bind and other transcription factors active in macrophage differentiation (Garg *et al*.,

2013). It was previously discovered that PMA activates the NOX complex. The activation can encourage the formation of $O_2^{\bullet-}$ on the inside of the cell. If SOD is active in the cell, the formation of $O_2^{\bullet-}$ can create H_2O_2 and $HO^{\bullet}$ (Auchère & Rusnak, 2002; Halliwell & Gutteridge, 2015; Pospíšil *et al*., 2019; Prasad *et al*., 2015; Prasad *et al*., 2016).

3. 5. 2 Confocal laser scanning microscopy

Confocal laser scanning microscopy is in recent years considered essential for biological research, as its techniques require less preparation when compared with electron microscopy for instance. It is one of the fluorescent imaging methods that is used nowadays (Canette & Briandet, 2014). The signal-to-background ratio is better than when using a conventional microscope (Sandison & Webb, 1994).

The basic concept for CLSM was developed by Dr. Marvin Minsky in the 1950s (Minsky, 1988). The method is based on imaging the focal plane of structures by scanning using laser excitation rather than full illumination, hence the name CLSM. The laser passes through and collects emitted photons of fluorophores within the sample (Kihm, 2011). These photons are collected pixel-by-pixel and, at the end, a picture of the necessary compartments is formed. The axial resolution is achieved through a pinhole, which rejects fluorescence emitted from other places than the sample plate. If a higher resolution is needed, a smaller pinhole is used. There is, however, a negative to using a smaller pinhole, as there is a smaller amount of signal that then reaches the detector and this loss cannot be compensated by increasing the laser light, as the laser will rather go through photobleaching and phototoxicity (Trinh & Fraser, 2015). This can become an advantage in some settings because opening the depth field results in the ability to capture cellular dynamics and trajectories, when the specimen being captured is three-dimensional (Kulesa & Fraser, 2000).

3. 5. 3 Western blotting

Western blotting is a method developed in the late 1970s. It is considered a fundamental technique for protein analysis because it is used to identify a specific protein from a sample containing a mixture of substances (Towbin *et al*., 1979). The method uses a two-dimensional polyacrylamide gel with the same spatial arrangement and transfers the proteins in the gel to a membrane, be it nitrocellulose or (full form) PVDF (polyvinylidene fluoride) (Alegria-Schaffer *et al*., 2009). The transfer process is done by electric forces or pressure, that transfer the proteins from gel to membrane (Spillman *et al*., 2007). The transferred proteins are then blocked and incubated with antibodies, that recognize a specific protein on the membrane.

This process uses two antibodies, a primary antibody, specific for the recognised protein and a secondary antibody, which recognises the primary antibody and is also capable of being imaged in some way, usually conjugated to an enzyme, such as horseradish peroxidase (HRP), which can then be imaged (Xie *et al*., 2017).

4. MATERIALS AND METHODS

4. 1 Biological material

- U-937 cell line (ATCC® CRL-1593.2™)

4. 2 Used chemicals, instruments, and solutions

4. 2. 1 Used chemicals

- RPMI-1640 w/ stable Glutamine (Biosera, # LM-R1639/500)
- Foetal bovine serum, Heat inactivated (FBS) (Biosera, # FB-1001H/500)
- Penicillin Streptomycin (Gibco, # 15140-122)
- Dimethyl sulfoxide (DMSO) (Duchefa Biochemie, # D1370.1000)
- Coomassie® Brilliant Blue G-250 (CBB) (Bio-Rad, # 1610406)
- Acetic Acid (Lach-Ner, # 607-002-00-6)
- Methanol
- Distilled water
- Ponceau S (Sigma-Aldrich, # P3504)
- Trypan Blue cell culture tested (Sigma-Aldrich, # T6146)
- Phorbol 12-myristate 13-acetate (Sigma-Aldrich, # P1586)
- Sodium chloride (Lach-Ner, #: 30093-AP0)
- Potassium chloride (Sigma-Aldrich, #: P9541)
- Di-sodium hydrogen phosphate dodecahydrate (Lach-Ner, #: 30061-CP0)
- Potassium dihydrogen phosphate (Sigma-Aldrich, #: P0662)
- PBS tablets (Gibco, # 18912-014)
- Acrylamide (Sigma-Aldrich, # A8887)
- N, N´-Methylene-Bis-Acrylamide (BIS) (Bio-Rad, # 1610200)
- Tris (Roche, # 10708976001)
- SDS (Bio-Rad, # 1610302)
- Urea (Lach-Ner, #: 40096-AP0)
- Glycerol anhydrous (Lach-Ner, #: 40058-AT0)
- Ammonium persulfate (APS) (Bio-Rad, # 161-0700)
- N,N,N´,N´- Tetramethylenediamine (TEMED) (Sigma-Aldrich, # T7024)
- 2-propanol
- 10% NP-40, Detergent, 10% solution in water (abcam, # ab142227)
- cOmplete™, Mini Protease Inhibitor Cocktail (Roche, # 4693124001)
- Phosphatase Inhibitor Cocktail (Sigma-Aldrich, # P0044)

- Tricine (Sigma-Aldrich, # T0377)
- PageRuler Plus Prestained Protein Ladder (ThermoScientific, # 26625)
- Tween 20 (Sigma-Aldrich, # 93773)
- Transfer Turbo 5x Transfer buffer (Bio-Rad, # 10026938)
- Albumin Fraction V, NZ-Origin (BSA) (Carl Roth, # 9048-46-8)
- Bromphenol Blue (Sigma-Aldrich, # 93773)
- DL- Dithiothreitol (DTT)(Sigma-Aldrich, # 43815)
- Anti-NADPH oxidase 4 antibody (anti-NOX4) (abcam, # ab133303)
- Anti- Malondialdehyde antibody (anti-MDA) (abcam, # ab27642)
- EIA Grade Affinity Purified Goat Anti-Rabbit IgG (H+L) Horseradish Peroxidase Conjugate (Bio-Rad, # 172-1019)
- FM™ 4-64 Dye (*N*-(3-Triethylammoniumpropyl)-4-(6-(4-(Diethylamino) Phenyl) Hexatrienyl) Pyridinium Dibromide) (ThermoScientific, # T3166)
- Hoechst 33342, Trihydrochloride, Trihydrate (ThermoScientific, # H3570)

4. 2. 2 Used kits

- Pierce™ BCA Protein Assay Kit (ThermoScientific, # 23227)
- Abcam™ MTT Assay Kit (Cell Proliferation) (abcam, # ab211091)
- Immobilon Western Chemiluminescent HRP Substrate (Merck Millipore, # WBKLS0500)

4. 2. 3 Used solutions and their preparation

- RPMI-1640 complete media: 500 ml PRMI-1640 + 50 ml FBS + 5 ml Penicillin Streptomycin
- RPMI-1640 serum free media: 500 ml RPMI-1640 + 5 ml Penicillin Streptomycin
- AB-3: 48 g Acrylamide + 1.5 g BIS dissolved in 100 ml of dH_2O
- Gel Buffer: 36.3 g Tris-base + 0.3 g SDS + 36 g Urea dissolved in 100 ml of dH_2O
- 10% APS
- 4% Stacking gel: 1 ml AB-3 + 3 ml Gel Buffer + 7.9 ml dH_2O + 110 µl 10% APS + 9 µl TEMED
- 10% Resolving gel: 3 ml AB-3 + 5 ml Gel Buffer + 1.5 ml glycerol + 5.4 ml dH_2O + 97 µl 10% APS + 7.5 µl TEMED
- Cathode Buffer 10x: 60.5 g Tris-base + 90 g Tricine + 5 g SDS dissolved in 1000 ml of dH_2O
- Anode Buffer 10x: 121 g Tris-base dissolved in 1000 ml of dH_2O

- RIPA Buffer: 150 mM $NaCl^-$ + pH 8.0 Tris + 0.1% SDS + 1% NP-40 + 1x Roche protease inhibitor cocktail + 1x Phosphatase inhibitor
- Loading Dye 5x: 100 mM DTT + 250 mM Tris-Cl^- + 8% SDS + 0.1% Bromphenol Blue + 40% Glycerol
- CBB Staining Solution: 100 mg CBB + 22.5 ml methanol + 22.5 ml dH_2O + 5 ml acetic acid
- CBB Destaining Solution: 125 ml dH_2O + 100 ml methanol + 25 ml acetic acid
- Ponceau S stain: 100 mg Ponceau S + 5 ml glacial acetic acid + 95 ml dH_2O
- PBS 10x: 80 g $NaCl^-$ + 2 g KCl^- + $Na_2HPO_4 \cdot 12\ H_2O$ + 2.4 ml KH_2PO_4 adjust to pH 7.4 dissolved in 1000 ml of dH_2O
- PBS 1x
- PBST 1x: 1 ml Tween-20 + 100 ml PBS 10x + 900 ml H_2O
- TBS 10x: 60.5 g Tris + 87.6 $NaCl^-$ + 800 ml H_2O adjust to pH 7.5, add to 1000 ml
- TBST: 1 ml Tween-20 + 100 ml TBS 10x + 900 ml H_2O
- Anti-MDA Primary antibody solution: 10 µl anti-MDA primary antibody + 2.5 g BSA + 49.99 ml TBST
- Anti-NOX4 Primary antibody solution: 5 µl anti-NOX4 primary antibody + 2.5 g BSA + 49.995 ml PBST
- Transfer Buffer: 19.35 g Tris-base + 3 ml acetic acid dissolved in 500 ml of dH_2O
- Transfer Turbo 1x Transfer Buffer
- Blocking solution: 1.25 g BSA + 20 ml PBST
- Goat anti-Rabbit Secondary antibody solution: 5 µl Goat Anti-Rabbit IgG + 1.25 g BSA + 19.995 ml PBST/19.995 ml TBST
- 0.05% Trypan Blue stain
- HRP probe 1:2 ratio: 500 µl HRP Substrate luminol reagent + 1000 µl HRP Peroxide substrate solution
- HRP probe 1:1 ratio: 750 µl HRP Substrate luminol reagent + 750 µl HRP Peroxide substrate solution

4. 3 List of used instruments and tools

- Biological Thermostat BT 120 (Laboratorní přístroje Praha, Czech Republic)
- TC20 Automated Cell Counter (Bio-Rad, USA)
- Vortex 4 basic (IKA, China)
- Laminar Box SCS Evo II. Class Biohazards (Merci, Czech Republic)

- Cell Culture CO_2 Incubator Mitre 4000 Series (Contherm, United Kingdom)
- Semi-automatic pipette Controller Swiftpet PRO (Corning HTL S.A., Poland)
- Magnetic Stirrer Color Squid IKAMAG® (IKA, China)
- Magnetic Stirrer with a heating plate C-MAG HS 7 (IKA, China)
- Programmable digital Rocker with platform RK-2D (Witeg, Germany)
- Fischerbrand™ Mini-Centrifuge 100-240V (Fisher Scientific, USA)
- ABT Analytical balances (Kern, Germany)
- EMB Precision Balance Scales (Kern, Germany)
- Dry Block Thermostat Bio-TDB-100 (BioSan, Latvia)
- PHMT Thermo-Shaker with a dry block (Grant-Bio, United Kingdom)
- Dry Bath Incubator (Major Science, Taiwan)
- Transsonic T460/H Ultrasonic Cleaning Tank (Elma, Germany)
- Trans-Blot® Turbo Transfer System (Bio-Rad, USA)
- Benchtop Centrifuge 5430R with rotary knobs (Eppendorf, Germany)
- Benchtop Centrifuge Sigma 3-30K (Sigma Centrifuges, Germany)
- Compact ultrasonic processor UP100H (Hielscher, Germany)
- Mini PROTEAN® Tetra System (Bio-Rad, USA)
- PowerPac Universal Power Suply (Bio-Rad, USA)
- PowerPac 1000 Power Suply (Bio-Rad, USA)
- mA700 Essential Power Supply (Merck Millipore, USA)
- Luminescent Image Analyzer Amersham Imager 600 (GE Healthcare Bio-Sciences AB, USA)
- Agilent BioTek Synergy Mx Monochromator-Based Multi-Mode Reader with Time-resolved Fluorescence (Bio-Tek, USA)
- CryoCube F740 Freezer (Eppendorf, Germany)
- Freezer BoxLGex 3410 MedLineG 5216 (Liebherr, Germany)
- Manual Autoclave 2340M (Tuttnauer, USA)
- Lab pH Meter inoLab® pH 7110 (WTW, Germany)
- Fluorescence microscope IX80 (Olympus Czech Group, Czech Republic)

4. 4 Methods

4. 4. 1 Cell Culture

The U-937 cell line was obtained from the Department of Immunology, Faculty of Medicine and Dentistry, Palacký University, Olomouc, Czech Republic. Cells were cultivated in complete RPMI-1640 supplemented with antibiotics, FBS and L-glutamine. The cells were then cultivated in an incubator in a 5% CO_2 atmosphere at 37ºC. These conditions correlate with human body conditions. The cells were passaged roughly every 4-7 days by adding 500 µl of the parent cell culture to a new 10 ml of complete RPMI-1640.

4. 4. 2 Seeding U-937 cells with different concentrations of PMA

The cell line was treated in 6-well plates. Into each plate, 0.5 ml of cell culture was mixed with 2.5 ml of complete RPMI-1640. In each well were then added different volumes of PMA so that the final concentrations of PMA in the wells are 50 nM, 100 nM, 250 nM, and 500 nM. As a negative control, no PMA was added, and as a positive control, DMSO was added in a concentration corresponding to the highest concentration of PMA since DMSO served as a solvent for PMA. The 6-well plate was then incubated at 37ºC in a 5% CO_2 atmosphere for 72 h and the cells were kept to differentiate.

4. 4. 3 Cell morphology using Confocal Laser Scanning Microscopy

The morphology of the cell culture was visualized using CLSM following the 72 h of differentiation.

For visualisation, the cells were washed with 1x PBS buffer at 2,000 rpm for 30 s. The cells were then co-stained for 5 min using FM-64 and Hoechst 33342. The prepared samples were then put on glass plates and scanned using a Fluorview 1000 confocal unit attached to an IX80 microscope. For the excitation of FM4-64, a 543 nm He-Ne laser was used, and its emission was detected by a 655-755 nm filter. Hoechst 33342 stain was excited using a 405-nm diode laser and its emission were detected within 430-470 nm.

4. 4. 4 Determination of the U-937 cell line viability using Trypan blue

To get a better understanding of cell culture proliferation, the growth curve was measured. Cells were counted every day at the same time each day for 25 days. The growth curve was measured by a Trypan blue viability test. This test is based on the principle that trypan blue only stains dead cells, thus distinguishing alive cells. For the test, 10 µl of cell culture was mixed with 2.5 µl, the final percentage of trypan blue was kept at 0.05%. After

2 minutes, the cells were inserted into a dual chamber cell counter, which was then placed on a cell counting machine TC20 for measurement. The cell numbers determined were then plotted against a number of days based.

4. 4. 5 Determination of the U-937 cell line viability using the MTT assay

The cell viability of the U-937 cell line was also determined by an MTT assay in addition to cell density in control and differentiated cells. MTT assay is based on the reduction that happens inside cells that reduces MTT forming yellow to purple formazan. This assay was conducted using an MTT assay kit. For the MTT assay, the cells were plated in a 24-well plate. Measurement was done in triplicates. To determine how many cells to use for the final test, cells were counted using a trypan blue test and 80,000 cells were pipetted for each individual test. Following this step, the cells were centrifuged at 2,500 rpm at 4ºC for 5 min. The cells were then resuspended in 50 µl of serum-free RPMI-1640 medium and 50 µl MTT reagent (room temperature) was pipetted into a 96-well plate. As a control for the MTT assay, serum-free RPMI-1640 was mixed with an MTT reagent and no cells. The 96-well plate was then covered with an aluminium foil and incubated at 37ºC for 3 h. After incubation, 150 µl of MTT solvent was added to each well and thoroughly mixed. Finally, the plate was put on a shaker for 15 minutes and was then measured spectrophotometrically at 590 nm. The calibration curve was prepared in Microsoft Excel and the viability of the sample cells was calculated.

4. 4. 6 Cell culture sample collection

Following incubation with PMA, the samples were harvested from the 6-well plate in 15 ml conical tubes and centrifuged for 10 min at 25°C for 1,400 rpm. The cells were suspended in 1x PBS and centrifuged for 10 min at 25ºC for 1,400 rpm. The washing was done twice to remove residual media to avoid any interference and the cells were then re-suspended as discussed in the next section.

4. 4. 7 Sample processing and protein estimation

The pelleted cells were re-suspended in a 1.5 ml centrifuge tube using 250 µl RIPA lysis buffer and left on ice for 5 minutes. The samples were then sonicated for 4 cycles of 20 seconds each at 40% amplitude. The samples were then left on the ice to rest for 5 minutes, and sonication was repeated. The samples were centrifuged at 14,000 rpm at 4ºC for 30 minutes. The supernatant was then transferred to a 1.5 ml centrifuge tube and stored in a freezer at -80°C until further use.

Protein concentration in harvested samples was estimated using a BCA protein assay kit. BCA reagent A was mixed with BCA reagent B in a 50:1 ratio to create a working reagent. Into a 96-well plate were added 10 µl of samples. Into another row were added protein standards provided with the BCA assay kit (concentrations 125 µg/ml, 250 µg/ml, 500 µg/ml, 750 µg/ml, 1,000 µg/ml, 1,500 µg/ml, and 2,000 µg/ml). As a control, RIPA buffer was added instead of the sample or standard. 200 µl of the working reagent was then added to each well. The 96-well plate was incubated in aluminium foil in an incubator for 30 minutes at 37ºC. The plate was then let to cool and measured spectrophotometrically at 562 nm. The calibration curve was prepared in Microsoft Excel and the protein concentration was calculated for electrophoresis and western blotting.

4. 4. 8 SDS-PAGE Electrophoresis

The volume of the isolated protein sample corresponding to 10 µg of proteins was transferred to a new centrifuge tube and mixed with RIPA buffer to a final volume of 20 µl. 5 µl of 5x Loading dye was then added and the samples were put on a dry thermal block at 70ºC for 10 minutes. After being cooled, the samples were loaded into a 1.5 mm polyacrylamide gel with 4% stacking gel and 12% resolving gel. The gels were self-prepared using the Bio-Rad Mini-PROTEAN® Tetra Cell system. 3 µl of PageRuler Plus Prestained Protein Ladder was used. Electrophoresis was performed at 50-75 mA for roughly 2.5 hours.

4. 4. 9 Gel Staining using Coomassie® Brilliant Blue

When the electrophoretic separation was complete, the gel was either used for transfer to a nitrocellulose membrane or stained with Coomassie® Brilliant Blue. The membrane was incubated in a CBB staining solution at room temperature on a shaker at 25 rpm for 40 minutes. The gel was destained using the CBB destaining solution 3-4 times for 15 minutes with repeated washing and then left for proper destaining overnight at 7 rpm. After destaining was complete, the gel was imaged using an Amersham 600 Imager.

4. 4. 10 Protein transfer and Western blotting

Protein transfer from the gel to the nitrocellulose membrane was done using Bio-Rad Trans-Blot® Turbo Transfer System. The transfer time was 10-20 minutes at 20-25 V. To determine the transferred proteins, the membrane was stained using Ponceau S stain. After washing, the transferred membrane was then left to block overnight at 4ºC in a PBST-BSA/TBST-BSA solution.

The blocked membrane was after overnight blocking incubated at room temperature in a primary antibody solution (anti-MDA/anti-NOX4) and left treated on a shaker with 25 rpm for 60 minutes. The membrane was washed 3 times in PBST/TBST on a shaker at 20 rpm, each for 10 minutes. The membrane was then incubated with an anti-rabbit secondary antibody on a shaker at 25 rpm for 60 minutes. After this incubation, the membrane was washed 3 times in PBST/TBST on a shaker (20 rpm). Following the final wash, the membrane was imaged using an Amersham 600 Imager and Immobilon Western Chemifluorescent HRP Substrate. The blots were then processed using ImageJ software.

5. RESULTS

5. 1 Growth curve of U-937 cell line and its viability

The growth curve of the U-937 cell line was prepared as described in Chapter 4.4.4. Figure 6 shows the growth curve for 25 days. The lag phase of the cell line was observed from day 0 to day 3. On the 7th day, the cells went through the exponential growth phase, the cells rapidly replicated during this time. The viability also stayed between 85% and 95%. From day 8 to day 15 the number of live cells remained roughly constant, the cell line thus entered another lag phase. After day 15 the number of live cells started to rapidly decrease and the cell line went through a decline/death phase. On the final day of the counting, the viability was around 7%.

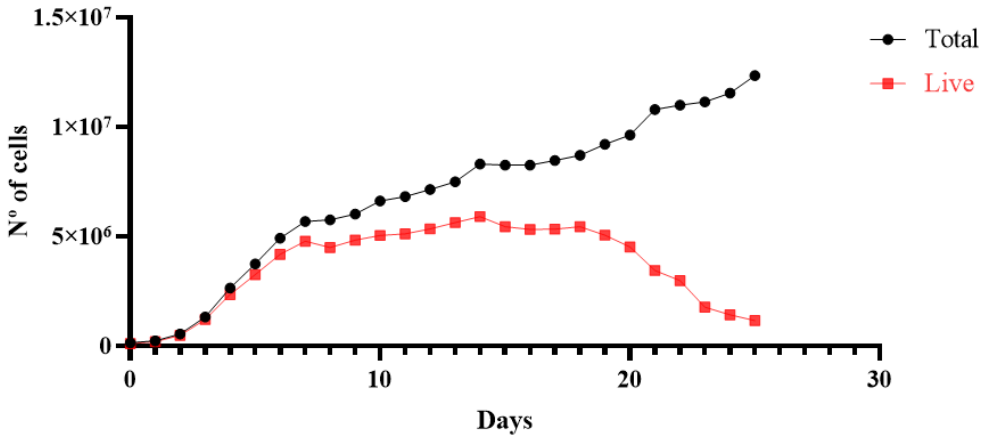

Figure 6: Cell growth curve measured for 25 days. Data points were collected each day at the same time.

To get a better understanding of viability, the growth curve was altered to a slope graph in Figure 7. The figure also shows the standard deviation measured in biological replicates (n=2).

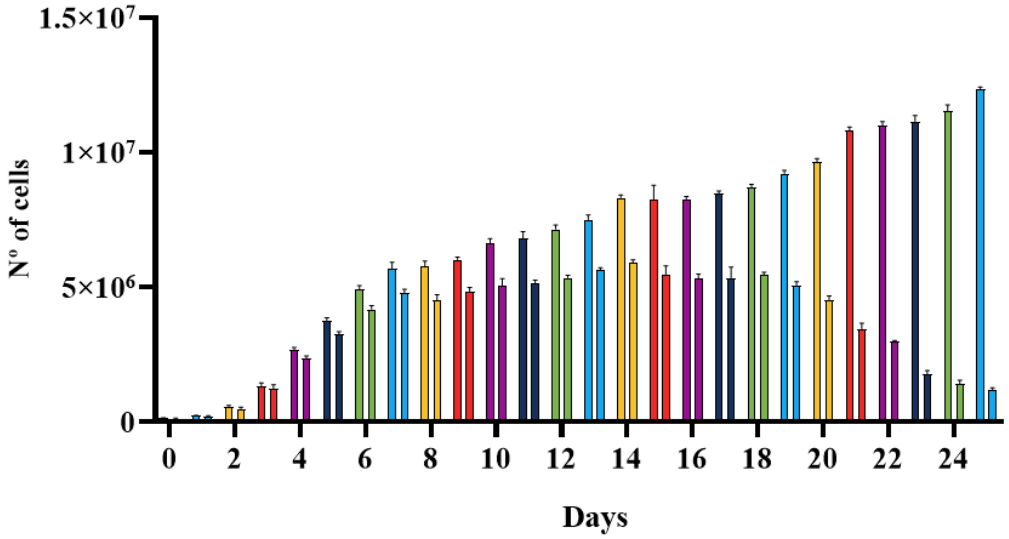

Figure 7: Cell growth curve measured for 25 days. Data points were collected every day at the same time. The standard deviation is shown at the top of each column. First column shows total cell amount, second column shows live cells.

For further experiments and cell differentiation, cells from days 3 and 4 of the growth curve were harvested.

The cell viability of the cell line was also tested on cells treated with different concentrations of PMA. The viability of different concentrations of PMA was tested using two different methods, both described in the following chapters 4.4.4 and 4.4.5, respectively. Figure 8 shows the cell viability under different concentrations of PMA using the Trypan blue test, while Figure 9 shows the cell viability of the different cells differentiated in PMA concentration using an MTT assay.

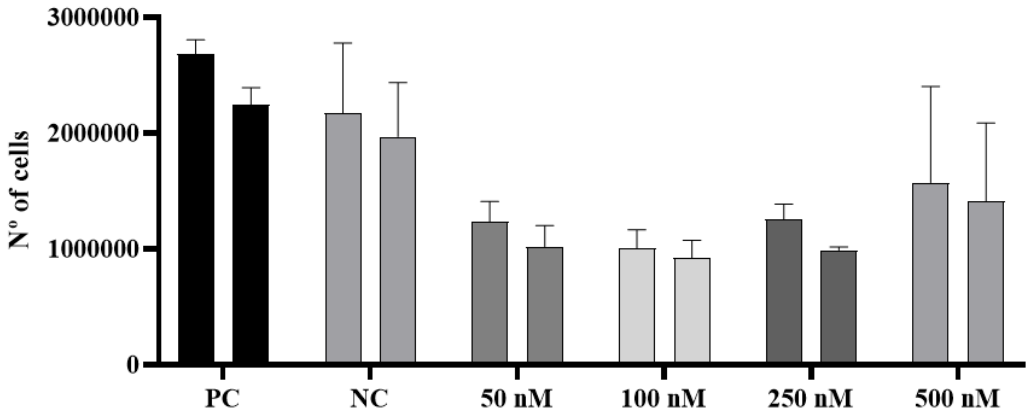

Figure 8: Cell viability of U-937 cells differentiated using different concentrations of PMA determined by the Trypan blue test. The standard deviation is shown at the top of each column. [PC- positive control, NC- negative control].

The viability determined by Trypan blue is the lowest in the 250 nM concentration, then 50 nM, negative control, 500 nM, positive control, and the highest viability was observed at 100 nM PMA concentration.

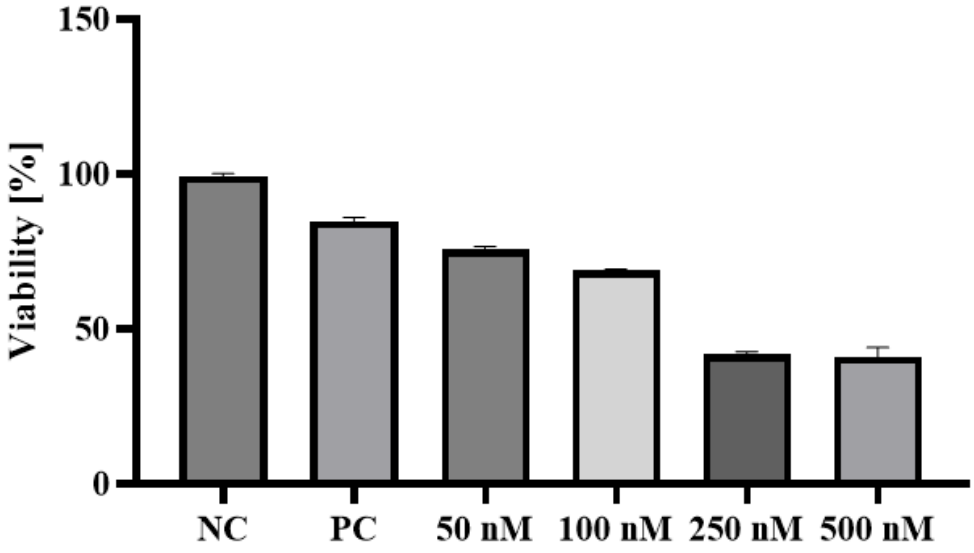

Figure 9: Cell viability of U-937 cells differentiated using different PMA concentrations determined by the MTT assay. The standard deviation is shown at the top of each bar. The standard deviation is shown at the top of each column [PC- positive control, NC- negative control].

For cell viability using MTT, the negative control was taken as a base for the test, counting it as 100%. Based on this consideration, all other viabilities were calculated. It was observed that viability decreases with the increasing concentration of PMA.

Comparing Figure 8 and Figure 9, there is a difference in ratios between the values of the same concentrations. Whereas the viability slightly decreases with increasing PMA concentration in the MTT assay, the slopes vary more in the viability test when Trypan Blue was used. This can be considered as the variations due to methodological differences.

5. 2 Morphology of the U-937 cell line differentiated in different PMA concentrations using confocal laser scanning microscopy

Samples for CLSM were prepared as described in Chapter 4.4.3.

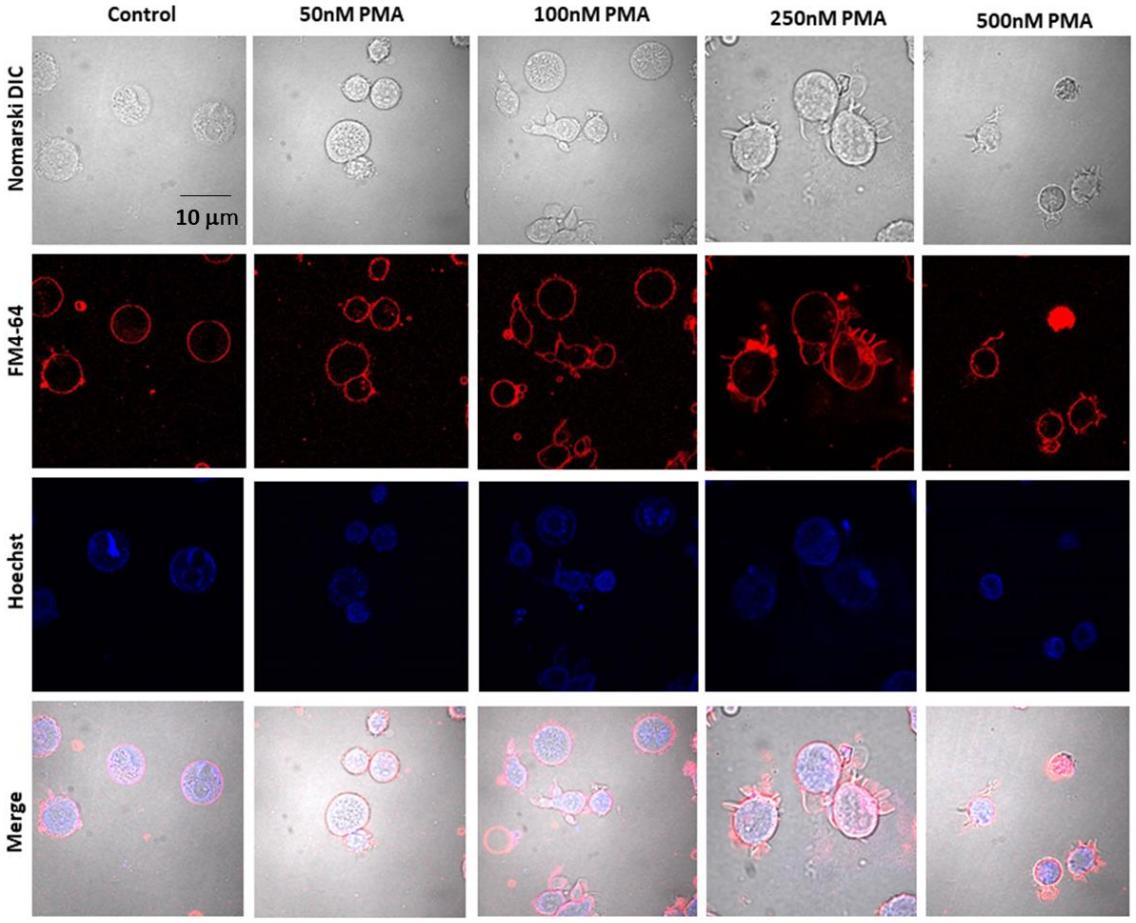

Figure 10: Images of U-937 cell line showing cells morphology differentiated using different PMA concentrations in comparison to control (please see descriptions within the images). From top to bottom are Normanski DIC , FM4-64 Hoechst 33343, and merged (FM4-64 and Hoechst 33343).

From the images acquired from the CLSM can be seen various altered morphological changes. Cellular integrity was confirmed using FM4-64, which stains cell membranes, and the nucleus dimension of the nucleus was stained with Hoechst 33343. While control cells show little to no differentiation, cells with increasing differentiation show more cell structures similar to macrophagic structures, such as pseudopodia. The nucleus also became larger as the PMA concentration increased to the point where the nucleus was as large as the entire cell.

5. 3 Immunoblotting

Protein samples were obtained as described in Chapter 4.4.7 and were separated using SDS-PAGE as described in Chapter 4.4.8. CBB staining was done as described in Chapter 4.4.9. Figure 11 shows the CBB staining of the obtained gel.

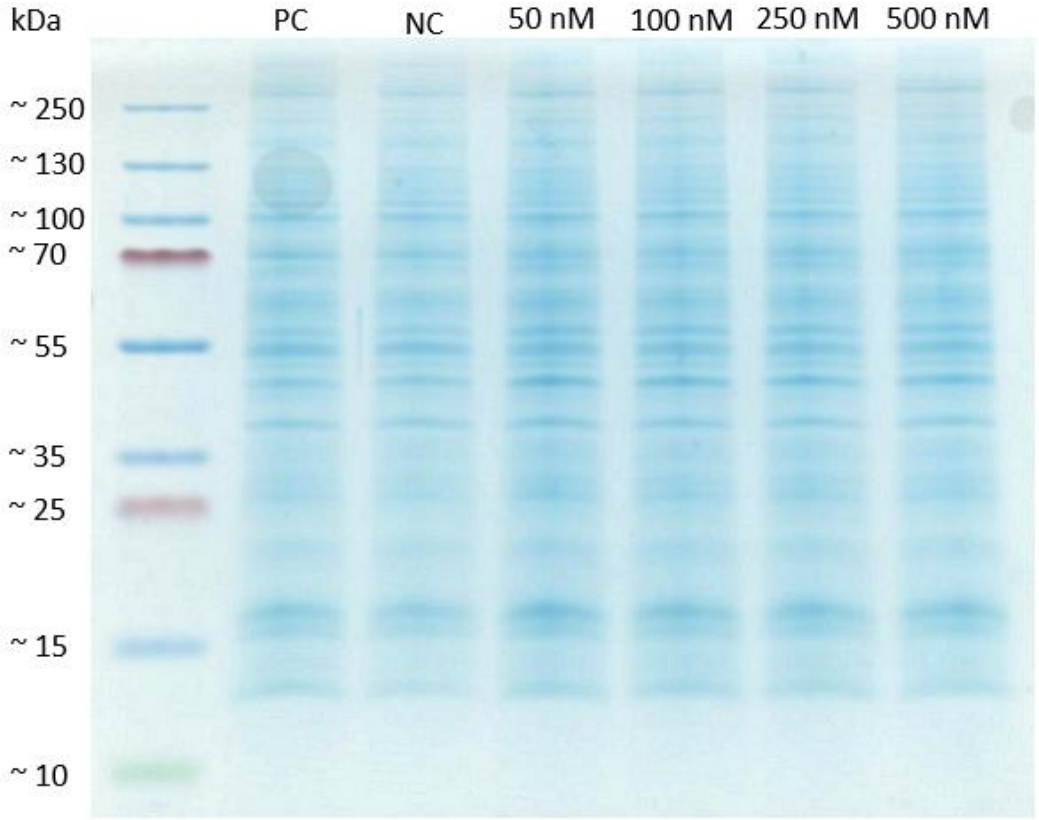

Figure 11: Image of CBB stained polyacrylamide gel separated by SDS-PAGE. Different concentrations of PMA used for differentiation are described above each assigned line. Molecular weights are shown on the left side of the membrane [PC- positive control, NC- negative control].

The results confirmed that protein concentration does not vary between differentiated and non-differentiated samples. The molecular weight of the proteins ranges from more than

250 kDa to about 13 kDa. This experiment was done to ensure that the starting protein concentration was not different.

Further, proteins were identified using the western blotting method. The steps of the method are described in Chapter 4.4.10. For the anti-MDA antibody, TBS and TBST buffers were used, whereas for the anti-NOX4, PBS and PBST were used. The result of the anti-MDA immunoblot is shown in Figure 12.

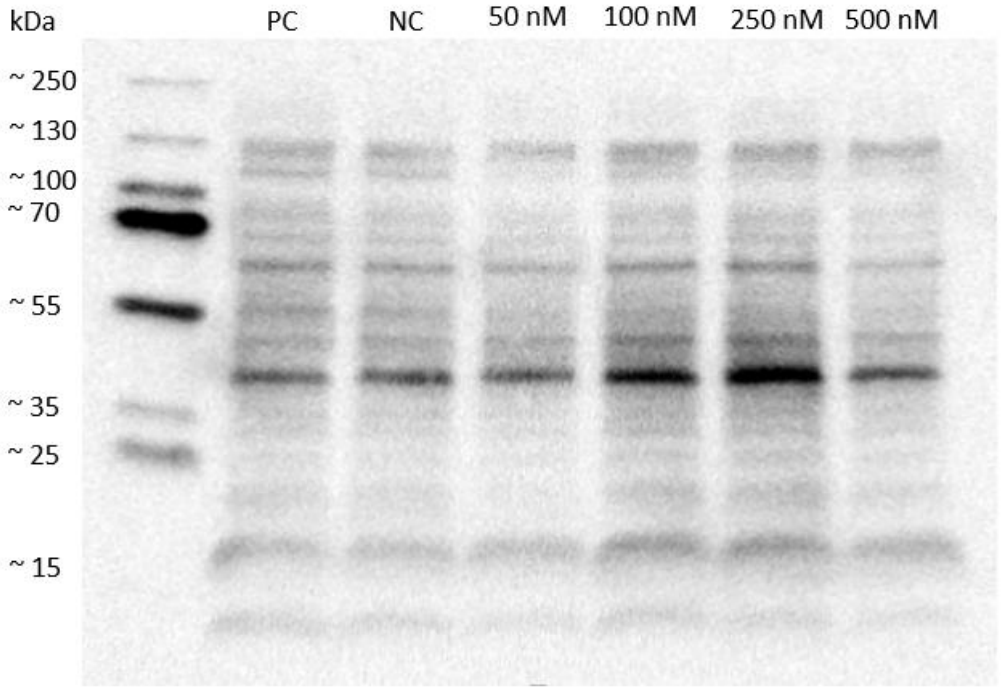

Figure 12: Image of nitrocellulose membrane with samples separated by SDS-PAGE. Western blot was performed using an anti-MDA primary antibody and imaging was performed using an HRP probe. Different PMA concentrations used for differentiation are described above each assigned line. Molecular weights showed on the left side of the membrane [PC- positive control, NC- negative control].

The immunoblot shows a significant increase of anti-MDA bands in cells differentiated at 100 nM and 250 nM. The biggest difference can be observed in the anti-MDA band around 40 kDa and 67 kDa.

The presented densitogram was prepared using ImageJ software. Please refer to results presented in Figure 13.

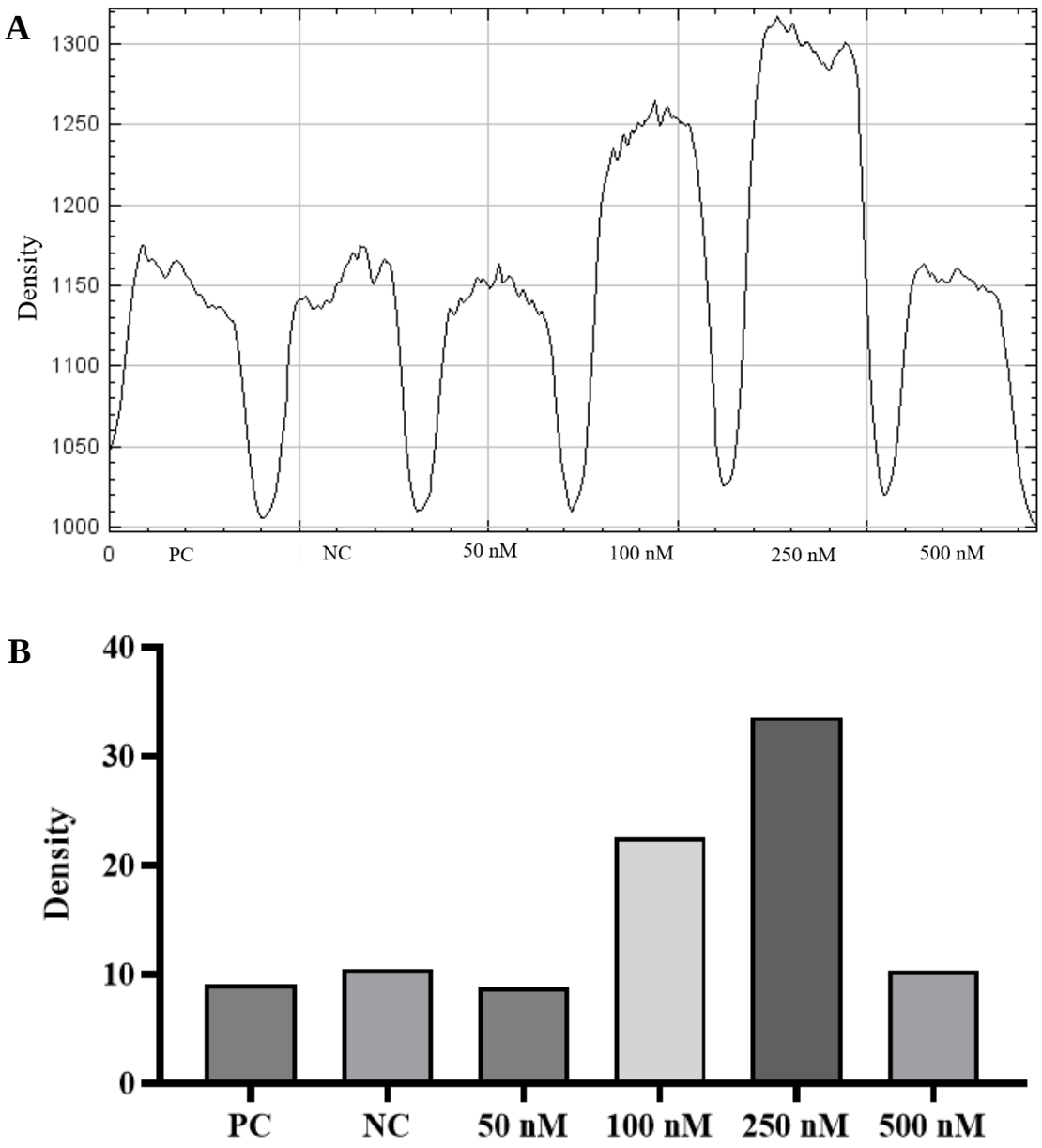

Figure 13: A: Profile obtained from the blot (lane corresponding to 40 kDa) showing of the membrane presented in Figure 12. B: Measured integrated density measured by the threshold of each blot of membrane shown in Figure 12. [PC- positive control, NC- negative control].

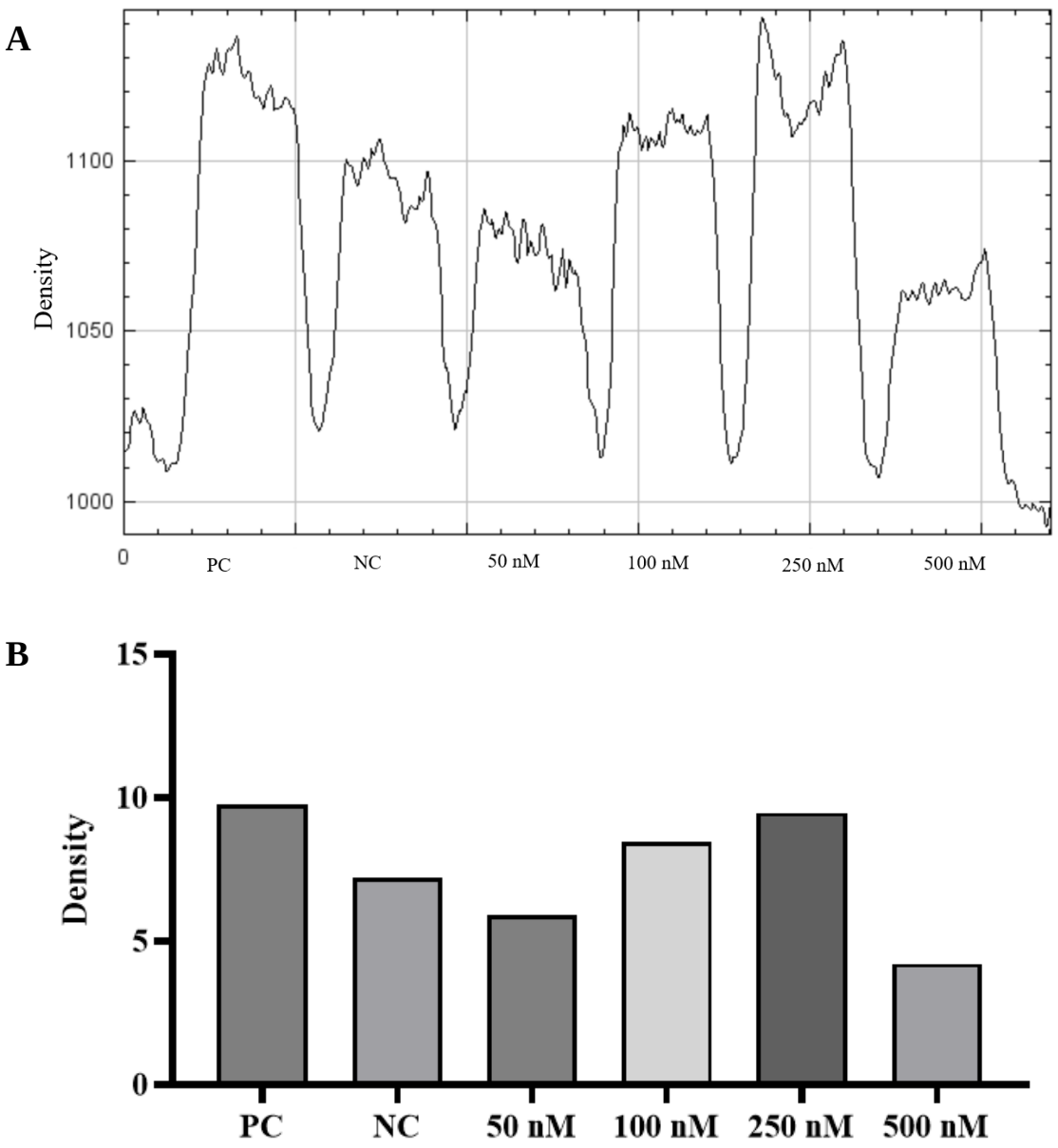

Figure 14 A: Profile obtained from the blot (lane corresponding to 65 kDa) showing of the membrane presented in Figure 12. B: Measured integrated density measured by the threshold of each blot of membrane shown in Figure 12. [PC- positive control, NC- negative control].

The following immunoblot with used anti-NOX4 primary antibody was used to identify NOX4 present and the result is presented in Figure 15.

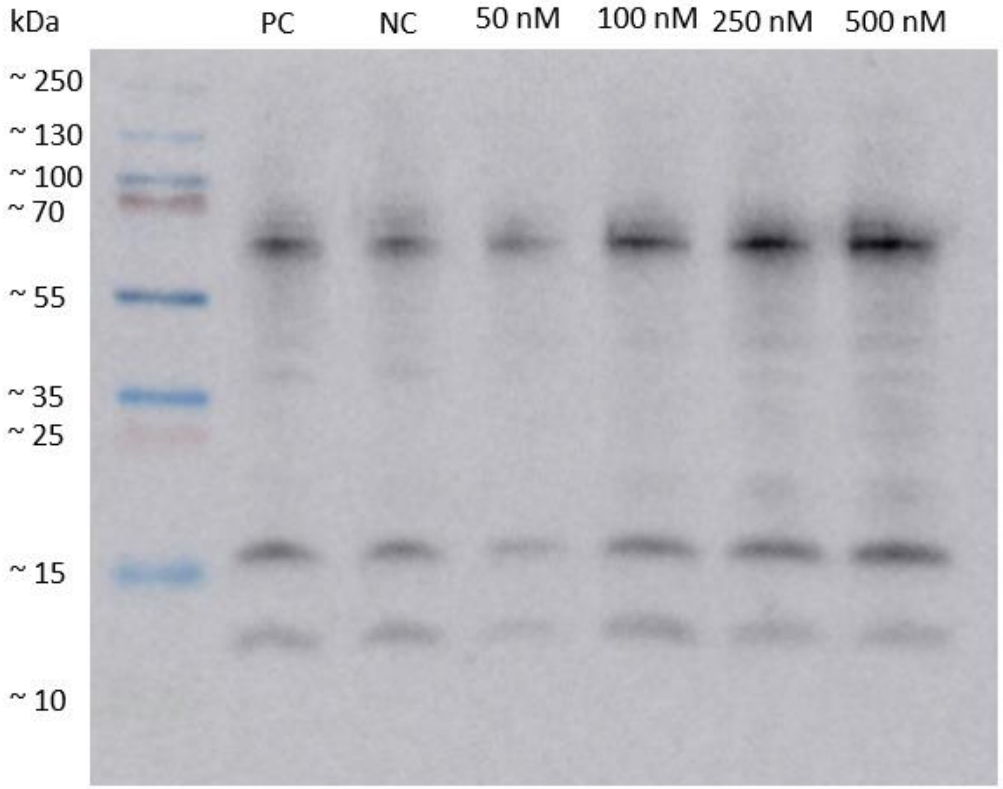

Figure 15: Western blot was performed using an anti-NOX4 primary antibody, imaging was performed using an HRP probe. Different PMA concentrations used for differentiation are described above each assigned line. Molecular weights showed on the left side of the membrane. [PC- positive control, NC- negative control].

The anti-NOX4 blots show an increase of NOX4 expression with increasing concentration of PMA. The bands assigned to NOX4 had a molecular weight of around 65 kDa. The controls show higher NOX4 expression than the 50 nM.

A densitogram that is presented was prepared using ImageJ and the result is presented as Figure 16.

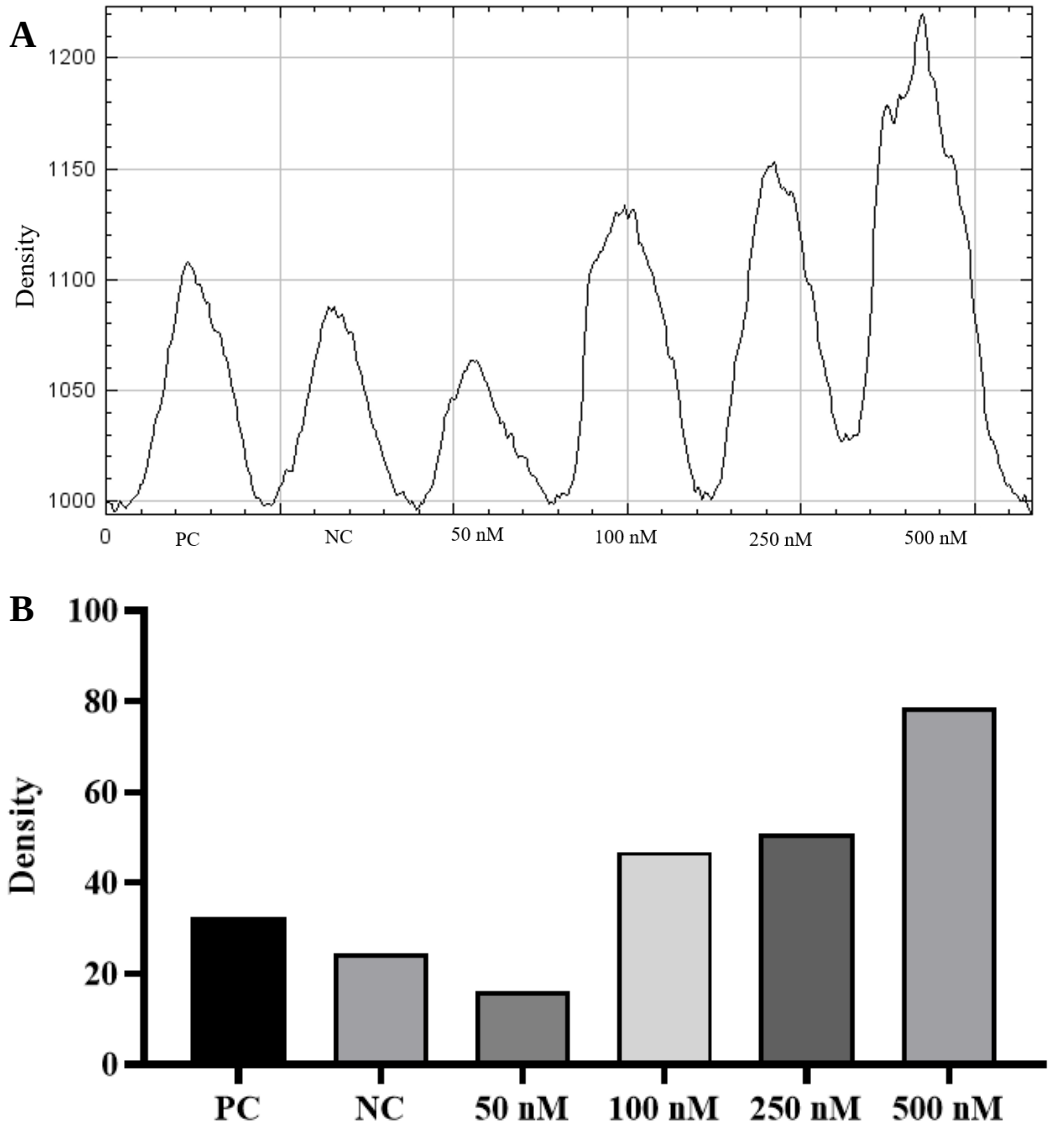

Figure 16: A: Profile of lane showing NOX4 expression presented in Figure 15. B: Measured integrated density measured by the threshold of each blot of membrane shown in Figure 15 [PC- positive control, NC- negative control].

6. DISCUSSION

As previously described in Chapter 5.1 the growth curve established that the cells go through a lag phase to day 2, then exponentially grow for some time, until day 7, when the number of live cells becomes stagnant. When the live cells become stagnant, the viability stayed around 60-80%. From day 15 onwards, the number of live cells rapidly decreased. Based on these numbers, we decided to harvest cells for further experiments always in the exponential growth phase, between days 3 – 10. Therefore, we harvested the cells on either day 3 or 4 when the viability was still greater than 90%. This also helped to limit the oversaturation of cells in further experiments. The viability measured after 72 h of differentiation allowed us to determine the upper limit of PMA to be used to differentiate the cells. The images obtained by CLSM (control sample) showed that the undifferentiated cells show morphology similar to monocytes. The non-differentiated cells also have a round shape and short microvilli, that appear also in lymphocytes (Majstoravich *et al*., 2004). The more differentiated the cells become, the more macrophage-like their morphology is. This morphology is seen in the form of long pseudopodia that are specific to the macrophage morphology (Sechi *et al*., 1997) and is usually seen in differentiated U-937 cells (Pagliara *et al*., 2005). Differentiated cells are also larger when compared to non-differentiated cells. In the 50 nM concentration, the cells have the same structure as the control cells. From this, we can deduce that no/minimum differentiation occurred under this condition. On the other hand, cells differentiated with 500 nM PMA appear smaller than the control cells and some even went through apoptosis. From this, we can deduce that this concentration is more damaging than the lower concentrations.

The western blotting results presented in Figure 12 shows that protein modification occurs the most in 100 nM and 250 nM PMA differentiated cells. This is in agreement with a previous report on cell differentiation (Prasad *et al*., 2021). This is also in agreement with the results obtained from CLSM where maximum differentiation can be seen at these concentrations while the 500 nM PMA can be seen to induce apoptosis in addition to cell differentiation. It has been previously reported that NADPH oxidase plays a huge role in the functioning of immune cells and their purpose in the immune system in general (Panday *et al*., 2014). The membrane in Figure 15 shows that there is an increasing expression of NOX4 at 100 and 250 nM PMA.

7. CONCLUSION

This thesis was focused on profiling proteins that may have some effect on processes that occur in monocyte differentiation. For the differentiation, the U-937 cell line was used, and the cell line was differentiated using different concentrations of PMA. We measured the results used in the thesis using CLSM and western blotting, the validation of these methods was done using different methods and pilot experiments were done prior to the protocol and experimental design. We report that during cell differentiation induced using PMA in this case, there is production of ROS which can lead to the formation of MDA by lipid peroxidation. MDA being reactive is able to interact with proteins and lead to its modification. In our experiments, we observed these modifications mostly around 40 kDa and 67 kDa. In addition, immunoblotting also indicated toward higher expression of NOX4 with certain concertation of PMA. The study is thus open for further investigation.

8. REFERENCES

Abo, A., Pick, E., Hall, A., Totty, N., Teahan, C. G., & Segal, A. W. (1991). Activation of the NADPH oxidase involves the small GTP-binding protein p21rac1. *Nature*, *353*(6345), 668–670.

Acharya, S., Peters, A. M., Norton, A. S., Murdoch, G. K., & Hill, R. A. (2013). Change in Nox4 expression is accompanied by changes in myogenic marker expression in differentiating C2C12 myoblasts. *Pflugers Archiv : European Journal of Physiology*, *465*(8), 1181–1196.

Ago, T., Kuroda, J., Pain, J., Fu, C., Li, H., & Sadoshima, J. (2010). Upregulation of Nox4 by hypertrophic stimuli promotes apoptosis and mitochondrial dysfunction in cardiac myocytes. *Circulation Research*, *106*(7), 1253–1264.

Akaike, T. (2001). Role of free radicals in viral pathogenesis and mutation. *Reviews in Medical Virology*, *11*(2), 87–101.

Alegria-Schaffer, A., Lodge, A., & Vattem, K. (2009). Chapter 33 Performing and Optimizing Western Blots with an Emphasis on Chemiluminescent Detection. *Methods in Enzymology*, *463*(C), 573–599.

Ambasta, R. K., Kumar, P., Griendling, K. K., Schmidt, H. H. H. W., Busse, R., & Brandes, R. P. (2004). Direct interaction of the novel Nox proteins with p22phox is required for the formation of a functionally active NADPH oxidase. *The Journal of Biological Chemistry*, *279*(44), 45935–45941.

Arbault, S., Pantano, P., Sojic, N., Amatore, C., Best-Belpomme, M., Sarasin, A., & Vuillaume, M. (1997). Activation of the NADPH oxidase in human fibroblasts by mechanical intrusion of a single cell with an ultramicroelectrode. *Carcinogenesis*, *18*(3), 569–574.

Auchère, F., & Rusnak, F. (2002). What is the ultimate fate of superoxide anion in vivo? *Journal of Biological Inorganic Chemistry*, *7*(6), 664–667.

Azumi, H., Inoue, N., Takeshita, S., Rikitake, Y., Kawashima, S., Hayashi, Y., Itoh, H., & Yokoyama, M. (1999). Expression of NADH/NADPH oxidase p22phox in human coronary arteries. *Circulation*, *100*(14), 1494–1498.

Babior, B. M. (1999). NADPH Oxidase: An Update. *Blood*, *93*(5), 1464–1476.

Bánfi, B., Maturana, A., Jaconi, S., Arnaudeau, S., Laforge, T., Sinha, B., Ligeti, E., Demaurex, N., & Krause, K.-H. (2000). A Mammalian H+ Channel Generated Through Alternative Splicing of the NADPH Oxidase Homolog NOH-1. *Science*, *287*(5450), 138–142.

Bánfi, B., Molnár, G., Maturana, A., Steger, K., Hegedûs, B., Demaurex, N., & Krause, K. H. (2001). A Ca(2+)-activated NADPH oxidase in testis, spleen, and lymph nodes. *The Journal of Biological Chemistry*, *276*(40), 37594–37601.

Barb, W. G., Baxendale, J. H., George, P., & Hargrave, K. R. (1951). Reactions of ferrous and ferric ions with hydrogen peroxide. Part I.—The ferrous ion reaction. *Transactions of the Faraday Society*, *47*(0), 462–500.

Batra, S., Cai, S., Balamayooran, G., & Jeyaseelan, S. (2012). Intrapulmonary administration of leukotriene B(4) augments neutrophil accumulation and responses in the lung to Klebsiella infection in CXCL1 knockout mice. *Journal of Immunology (Baltimore, Md. : 1950)*, *188*(7), 3458–3468.

Bedard, K., & Krause, K. H. (2007). The NOX family of ROS-generating NADPH oxidases: Physiology and pathophysiology. *Physiological Reviews*, *87*(1), 245–313.

Benjamin, J. T., Torres, B. A., & Maheshwari, A. (2018). Neonatal Leukocyte Physiology and Disorders. *Avery's Diseases of the Newborn, Tenth Edition*, 1187-1197.e4.

Bohle, A., Bader, R., Grund, K. E., Mackensen, S., & Neunhoeffer, J. (1977). Serum creatinine concentration and renal interstitial volume. Analysis of correlations in endocapillary (acute) glomerulonephritis and in moderately severe mesangioproliferative glomerulonephritis. *Virchows Archiv. A, Pathological Anatomy and Histology*, *375*(2), 87–96.

Bureau, C., Bernad, J., Chaouche, N., Orfila, C., Béraud, M., Gonindard, C., Alric, L., Vinel, J. P., & Pipy, B. (2001). Nonstructural 3 protein of hepatitis C virus triggers an oxidative burst in human monocytes via activation of NADPH oxidase. *The Journal of Biological Chemistry*, *276*(25), 23077–23083.

Cai, Z. (2005). Lipid Peroxidation. *Encyclopedia of Toxicology*, 730–734.

Canette, A., & Briandet, R. (2014). MICROSCOPY | Confocal Laser Scanning Microscopy. *Encyclopedia of Food Microbiology: Second Edition*, 676–683.

Chakraborti, S., Roy, S., Mandal, A., Chowdhury, A., & Chakraborti, T. (2013). Role of PKC-ζ in NADPH oxidase-PKCα-Giα axis dependent inhibition of β-adrenergic response by U46619 in pulmonary artery smooth muscle cells. *Archives of Biochemistry and Biophysics*, *540*(1–2), 133–144.

Chanput, W., Peters, V., & Wichers, H. (2015). THP-1 and U937 cells. *The Impact of Food Bioactives on Health: In Vitro and Ex Vivo Models*, 147–159.

Chao, M. R., Evans, M. D., Hu, C. W., Ji, Y., Møller, P., Rossner, P., & Cooke, M. S. (2021). Biomarkers of nucleic acid oxidation – A summary state-of-the-art. *Redox Biology*, *42*, 101872.

Cheignon, C., Faller, P., Testemale, D., Hureau, C., & Collin, F. (2016). Metal-catalyzed oxidation of Aβ and the resulting reorganization of Cu binding sites promote ROS production. *Metallomics : Integrated Biometal Science*, *8*(10), 1081–1089.

Chen, L., Hou, X., Xiao, J., Kuroda, J., Ago, T., Sadoshima, J., Cohen, R. A., & Tong, X. Y. (2014). Both hydrogen peroxide and transforming growth factor beta 1 contribute to endothelial Nox4 mediated angiogenesis in endothelial Nox4 transgenic mouse lines. *Biochimica et Biophysica Acta*, *1842*(12 Pt A), 2489–2499.

Chun, E. M., Park, Y. J., Kang, H. S., Cho, H. M., Jun, D. Y., & Kim, Y. H. (2001). Expression of the apolipoprotein C-II gene during myelomonocytic differentiation of human leukemic cells. *Journal of Leukocyte Biology*, *69*(4), 645–650.

Clark, R. A., Volpp, B. D., Leidal, K. G., & Nauseef, W. M. (1990). Two cytosolic components of the human neutrophil respiratory burst oxidase translocate to the plasma membrane during cell activation. *The Journal of Clinical Investigation*, *85*(3), 714–721.

Dahan, I., Issaeva, I., Gorzalczany, Y., Sigal, N., Hirshberg, M., & Pick, E. (2002). Mapping of functional domains in the p22(phox) subunit of flavocytochrome b(559) participating in the assembly of the NADPH oxidase complex by "peptide walking." *The Journal of Biological Chemistry*, *277*(10), 8421–8432.

Das, T. K., Mas, ;, Wati, R., Kaneez Fatima-Shad, ;, & Fatima-Shad, K. (2015). Oxidative Stress Gated by Fenton and Haber Weiss Reactions and Its Association With Alzheimer's Disease. *Archives of Neuroscience 2015 2:2*, *2*(2), 20078.

De Deken, X., Wang, D., Many, M. C., Costagliola, S., Libert, F., Vassart, G., Dumont, J. E., & Miot, F. (2000). Cloning of two human thyroid cDNAs encoding new members of the NADPH oxidase family. *The Journal of Biological Chemistry*, *275*(30), 23227–23233.

de Souza, A. W. S., de Melo Cruvinel, W., & Andrade, L. E. C. (2022). Targeting macrophages in systemic diseases. *Macrophages in the Human Body: A Tissue Level Approach*, 279–302.

DeCoursey, T. E., Cherny, V. V., Morgan, D., Katz, B. Z., & Dinauer, M. C. (2001). The gp91phox Component of NADPH Oxidase Is Not the Voltage-gated Proton Channel in Phagocytes, but It Helps. *Journal of Biological Chemistry*, *276*(39), 36063–36066.

Del Rio, D., Stewart, A. J., & Pellegrini, N. (2005). A review of recent studies on malondialdehyde as toxic molecule and biological marker of oxidative stress. *Nutrition, Metabolism, and Cardiovascular Diseases : NMCD*, *15*(4), 316–328.

DeLeo, F. R., Allen, L.-A. H., Apicella, M., & Nauseef, W. M. (1999). NADPH Oxidase Activation and Assembly During Phagocytosis. *The Journal of Immunology*, *163*(12), 6732–6740.

Dikalov, S. (2011). Crosstalk between mitochondria and NADPH oxidases. *Free Radical Biology & Medicine*, *51*(7), 1289.

Dupuy, C., Ohayon, R., Valent, A., Noël-Hudson, M. S., Dème, D., & Virion, A. (1999). Purification of a novel flavoprotein involved in the thyroid NADPH oxidase. Cloning of the porcine and human cdnas. *The Journal of Biological Chemistry*, *274*(52), 37265–37269.

Edens, W. A., Sharling, L., Cheng, G., Shapira, R., Kinkade, J. M., Lee, T., Edens, H. A., Tang, X., Sullards, C., Flaherty, D. B., Benian, G. M., & David Lambeth, J. (2001). Tyrosine cross-linking of extracellular matrix is catalyzed by Duox, a multidomain oxidase/peroxidase with homology to the phagocyte oxidase subunit gp91phox. *The Journal of Cell Biology*, *154*(4), 879–891.

El Hassani, R. A., Benfares, N., Caillou, B., Talbot, M., Sabourin, J. C., Belotte, V., Morand, S., Gnidehou, S., Agnandji, D., Ohayon, R., Kaniewski, J., Noël-Hudson, M. S., Bidart, J. M., Schlumberger, M., Virion, A., & Dupuy, C. (2005). Dual oxidase2 is expressed all along the digestive tract. *American Journal of Physiology. Gastrointestinal and Liver Physiology*, *288*(5).

Esterbauer, H., & Cheeseman, K. H. (1990). Determination of aldehydic lipid peroxidation products: malonaldehyde and 4-hydroxynonenal. *Methods in Enzymology*, *186*(C), 407–421.

Esterbauer, H., Schaur, R. J., & Zollner, H. (1991). Chemistry and biochemistry of 4-hydroxynonenal, malonaldehyde and related aldehydes. *Free Radical Biology & Medicine*, *11*(1), 81–128.

Evangelista, A. M., Thompson, M. D., Bolotina, V. M., Tong, X., & Cohen, R. A. (2012). Nox4- and Nox2-dependent oxidant production is required for VEGF-induced SERCA cysteine-674 S-glutathiolation and endothelial cell migration. *Free Radical Biology & Medicine*, *53*(12), 2327–2334.

Feng, D., Yang, C., Geurts, A. M., Kurth, T., Liang, M., Lazar, J., Mattson, D. L., O'Connor, P. M., & Cowley, A. W. (2012). Increased expression of NAD(P)H oxidase subunit p67phox in the renal medulla contributes to excess oxidative stress and salt-sensitive hypertension. *Cell Metabolism*, *15*(2), 201.

Fink, M. P. (2003). Ethyl pyruvate: a novel anti-inflammatory agent. *Critical Care Medicine*, *31*(1 Suppl).

Frankel, E. N., & Neff, W. E. (1983). Formation of malonaldehyde from lipid oxidation products. *Biochimica et Biophysica Acta (BBA) - Lipids and Lipid Metabolism*, *754*(3), 264–270.

Fukata, M., Hernandez, Y., Conduah, D., Cohen, J., Chen, A., Breglio, K., Goo, T., Hsu, D., Xu, R., & Abreu, M. T. (2009). Innate immune signaling by Toll-like receptor-4 (TLR4) shapes the inflammatory microenvironment in colitis-associated tumors. *Inflammatory Bowel Diseases*, *15*(7), 997.

Gao, H. M., Zhou, H., & Hong, J. S. (2012). NADPH oxidases: novel therapeutic targets for neurodegenerative diseases. *Trends in Pharmacological Sciences*, *33*(6), 295–303.

Gardiner, G. J., Deffit, S. N., Mcletchie, S., Pérez, L., Walline, C. C., Blum, J. S., Santambrogio, L., & Einstein, A. (2013). *A role for NADPH oxidase in antigen presentation*.

Garg, R., Caino, M. C., & Kazanietz, M. G. (2013). Regulation of Transcriptional Networks by PKC Isozymes: Identification of c-Rel as a Key Transcription Factor for PKC-Regulated Genes. *PLOS ONE*, *8*(6), e67319.

Geiszt, M., Kopp, J. B., Várnai, P., & Leto, T. L. (2000). Identification of renox, an NAD(P)H oxidase in kidney. *Proceedings of the National Academy of Sciences of the United States of America*, *97*(14), 8010–8014.

Golubev, A., Khrustalev, S., & Butov, A. (2003). An in silico investigation into the causes of telomere length heterogeneity and its implications for the Hayflick limit. *Journal of Theoretical Biology*, *225*(2), 153–170.

Griendling, K. K., Sorescu, D., & Ushio-Fukai, M. (2000). NAD(P)H oxidase: role in cardiovascular biology and disease. *Circulation Research*, *86*(5), 494–501.

Gu, Y., Filippi, M. D., Cancelas, J. A., Siefring, J. E., Williams, E. P., Jasti, A. C., Harris, C. E., Lee, A. W., Prabhakar, R., Atkinson, S. J., Kwiatkowski, D. J., & Williams, D. A. (2003). Hematopoietic cell regulation by Rac1 and Rac2 guanosine triphosphatases. *Science (New York, N.Y.)*, *302*(5644), 445–449.

Haber, F., Weiss, J., Seph, J. O., & Eiss, W. (1934). The catalytic decomposition of hydrogen peroxide by iron salts. *Proceedings of the Royal Society of London. Series A - Mathematical and Physical Sciences*, *147*(861), 332–351.

Haber, F., & Willstätter, R. (1931). Unpaarigkeit und Radikalketten im Reaktionsmechanismus organischer und enzymatischer Vorgänge. *Berichte Der Deutschen Chemischen Gesellschaft (A and B Series)*, *64*(11), 2844–2856.

Hajjar, C., Cherrier, M. V., Mirandela, G. D., Petit-Hartlein, I., Stasia, M. J., Fontecilla-Camps, J. C., Fieschi, F., & Dupuy, J. (2017). The NOX Family of Proteins Is Also Present in Bacteria. *MBio*, *8*(6).

Halliwell, B., & Gutteridge, J. M. C. (2015). Free Radicals in Biology and Medicine. *Free Radicals in Biology and Medicine*.

Hansen, J. M., Go, Y. M., & Jones, D. P. (2006). Nuclear and mitochondrial compartmentation of oxidative stress and redox signaling. *Annual Review of Pharmacology and Toxicology*, *46*, 215–234.

Harper, A. M., Chaplin, M. F., & Segal, A. W. (1985). Cytochrome b-245 from human neutrophils is a glycoprotein. *Biochemical Journal*, *227*(3), 783.

Harper, R. W., Xu, C., Eiserich, J. P., Chen, Y., Kao, C. Y., Thai, P., Setiadi, H., & Wu, R. (2005). Differential regulation of dual NADPH oxidases/peroxidases, Duox1 and Duox2, by Th1 and Th2 cytokines in respiratory tract epithelium. *FEBS Letters*, *579*(21), 4911–4917.

Harper, R. W., Xu, C., McManus, M., Heidersbach, A., & Eiserich, J. P. (2006). Duox2 exhibits potent heme peroxidase activity in human respiratory tract epithelium. *FEBS Letters*, *580*(22), 5150–5154.

Hattori, H. (1961). Studies on the labile, stable Nadi oxidase and peroxidase staining reactions in the isolated particles of horse granulocyte. Nagoya J. Med. Sci. 1961, 23, 362–378.

Hayflick, L., & Moorhead, P. S. (1961). The serial cultivation of human diploid cell strains. *Experimental Cell Research*, *25*(3), 585–621.

Hecker, M., & Ullrich, V. (1989). On the mechanism of prostacyclin and thromboxane A2 biosynthesis. *Journal of Biological Chemistry*, *264*(1), 141–150.

Heinrich, F., Lehmbecker, A., Raddatz, B. B., Kegler, K., Tipold, A., Stein, V. M., Kalkuhl, A., Deschl, U., Baumgärtner, W., Ulrich, R., & Spitzbarth, I. (2017). Morphologic, phenotypic, and transcriptomic characterization of classically and alternatively activated canine blood-derived macrophages in vitro. *PLOS ONE*, *12*(8), e0183572.

Heyworth, P. G., Curnutte, J. T., Nauseef, W. M., Volpp, B. D., Pearson, D. W., Rosen, H., & Clark, R. A. (1991). Neutrophil nicotinamide adenine dinucleotide phosphate oxidase assembly. Translocation of p47-phox and p67-phox requires interaction between p47-phox and cytochrome b558. *The Journal of Clinical Investigation*, *87*(1), 352–356.

Hoff, P., & Buttgereit, F. (2014). NADPH oxidase 4 represents a potential target for the treatment of osteoporosis. *Cellular & Molecular Immunology 2014 11:4*, *11*(4), 317–319.

Irwin, M. E., Johnson, B. P., Manshouri, R., Amin, H. M., & Chandra, J. (2015). A NOX2/Egr-1/Fyn pathway delineates new targets for TKI-resistant malignancies. *Oncotarget*, *6*(27), 23631.

Italiani, P., & Boraschi, D. (2014). From monocytes to M1/M2 macrophages: Phenotypical vs. functional differentiation. *Frontiers in Immunology*, *5*(OCT), 514.

Jakubzick, C. V., Randolph, G. J., & Henson, P. M. (2017). Monocyte differentiation and antigen-presenting functions. *Nature Reviews. Immunology*, *17*(6), 349–362.

Kamdar, K., Nguyen, V., & DePaolo, R. W. (2013). Toll-like receptor signaling and regulation of intestinal immunity. *Virulence*, *4*(3), 207.

Kang, X., Wei, X., Wang, X., Jiang, L., Niu, C., Zhang, J., Chen, S., & Meng, D. (2016). Nox2 contributes to the arterial endothelial specification of mouse induced pluripotent stem cells by upregulating Notch signaling. *Scientific Reports 2016 6:1*, *6*(1), 1–13.

Kawahara, T., Kuwano, Y., Teshima-Kondo, S., Takeya, R., Sumimoto, H., Kishi, K., Tsunawaki, S., Hirayama, T., & Rokutan, K. (2004). Role of nicotinamide adenine dinucleotide phosphate oxidase 1 in oxidative burst response to Toll-like receptor 5 signaling in large intestinal epithelial cells. *Journal of Immunology (Baltimore, Md. : 1950)*, *172*(5), 3051–3058.

Kawai, T., & Akira, S. (2007). Signaling to NF-kappaB by Toll-like receptors. *Trends in Molecular Medicine*, *13*(11), 460–469.

Kehm, R., Baldensperger, T., Raupbach, J., & Höhn, A. (2021). Protein oxidation - Formation mechanisms, detection and relevance as biomarkers in human diseases. *Redox Biology*, *42*, 101901.

Kihm, K. D. (2011). Confocal Laser Scanning Microscopy (CLSM). *Near-Field Characterization of Micro/Nano-Scaled Fluid Flows*, 55–79.

Kikuchi, H., Hikage, M., Miyashita, H., & Fukumoto, M. (2000). NADPH oxidase subunit, gp91(phox) homologue, preferentially expressed in human colon epithelial cells. *Gene*, *254*(1–2), 237–243.

Kim, J. H., Song, S. Y., Park, S. G., Song, S. U., Xia, Y., & Sung, J. H. (2012). Primary Involvement of NADPH Oxidase 4 in Hypoxia-Induced Generation of Reactive Oxygen Species in Adipose-Derived Stem Cells. *Stem Cells and Development*, *21*(12), 2212.

Kim, Y. M., Kim, S. J., Tatsunami, R., Yamamura, H., Fukai, T., & Fukai, M. U. (2017). ROS-induced ROS release orchestrated by Nox4, Nox2, and mitochondria in VEGF signaling and angiogenesis. *American Journal of Physiology. Cell Physiology*, *312*(6), C749–C764.

Knaus, U. G., Heyworth, P. G., Evans, T., Curnutte, J. T., & Bokoch, G. M. (1991). Regulation of phagocyte oxygen radical production by the GTP-binding protein Rac 2. *Science (New York, N.Y.)*, *254*(5037), 1512–1515.

Korman, B. D., Huang, C. C., Skamra, C., Wu, P., Koessler, R., Yao, D., Huang, Q. Q., Pearce, W., Sutton-Tyrrell, K., Kondos, G., Edmundowicz, D., Pope, R., & Ramsey-Goldman, R. (2014). Inflammatory expression profiles in monocyte-to-macrophage differentiation in patients with systemic lupus erythematosus and relationship with atherosclerosis. *Arthritis Research and Therapy*, *16*(4), 1–12.

Kulesa, P. M., & Fraser, S. E. (2000). In ovo time-lapse analysis of chick hindbrain neural crest cell migration shows cell interactions during migration to the branchial arches. *Development (Cambridge, England)*, *127*(6), 1161–1172.

Kuroda, J., Ago, T., Matsushima, S., Zhai, P., Schneider, M. D., & Sadoshima, J. (2010). NADPH oxidase 4 (Nox4) is a major source of oxidative stress in the failing heart. *Proceedings of the National Academy of Sciences of the United States of America*, *107*(35), 15565–15570.

Kuroda, J., Nakagawa, K., Yamasaki, T., Nakamura, K. I., Takeya, R., Kuribayashi, F., Imajoh-Ohmi, S., Igarashi, K., Shibata, Y., Sueishi, K., & Sumimoto, H. (2005). The superoxide-producing NAD(P)H oxidase Nox4 in the nucleus of human vascular endothelial cells. *Genes to Cells : Devoted to Molecular & Cellular Mechanisms*, *10*(12), 1139–1151.

Lambert, A. J., & Brand, M. D. (2009). Reactive oxygen species production by mitochondria. *Methods in Molecular Biology (Clifton, N.J.)*, *554*, 165–181.

Laurindo, F. R. M., Araujo, T. L. S., & Abrahão, T. B. (2014). Nox NADPH Oxidases and the Endoplasmic Reticulum. *Antioxidants & Redox Signaling*, *20*(17), 2755.

Lee, H. S., Stachelek, S. J., Tomczyk, N., Finley, M. J., Composto, R. J., & Eckmann, D. M. (2013). Correlating macrophage morphology and cytokine production resulting from biomaterial contact. *Journal of Biomedical Materials Research. Part A*, *101*(1), 203–212.

Lee, J. E., Cho, K. E., Lee, K. E., Kim, J., & Bae, Y. S. (2014). Nox4-Mediated Cell Signaling Regulates Differentiation and Survival of Neural Crest Stem Cells. *Molecules and Cells*, *37*(12), 907.

Lendeckel, U., Venz, S., & Wolke, C. (2022). Macrophages: shapes and functions. *ChemTexts*, *8*(2), 1–12.

Li, G., Scull, C., Ozcan, L., & Tabas, I. (2010). NADPH oxidase links endoplasmic reticulum stress, oxidative stress, and PKR activation to induce apoptosis. *The Journal of Cell Biology*, *191*(6), 1113–1125.

Li, H., Liu, Q., Wang, N., & Xu, J. (2011). Correlation of different NADPH oxidase homologues with late endothelial progenitor cell senescence induced by angiotensin II: effect of telmisartan. *Internal Medicine (Tokyo, Japan)*, *50*(16), 1631–1642.

Li, R., Jia, Z., & Trush, M. A. (2016). Defining ROS in Biology and Medicine. *Reactive Oxygen Species (Apex, N.C.)*, *1*(1), 9.

Lin, C. C., Lee, I. T., Yang, Y. L., Lee, C. W., Kou, Y. R., & Yang, C. M. (2009). Induction of COX-2/PGE(2)/IL-6 is crucial for cigarette smoke extract-induced airway inflammation: Role of TLR4-dependent NADPH oxidase activation. *Free Radical Biology & Medicine*, *48*(2), 240–254.

Liochev, S. I., & Fridovich, I. (2002). The Haber-Weiss cycle -- 70 years later: an alternative view. *Redox Report : Communications in Free Radical Research*, *7*(1), 55–57.

Maitra, U., Singh, N., Gan, L., Ringwood, L., & Li, L. (2009). IRAK-1 Contributes to Lipopolysaccharide-induced Reactive Oxygen Species Generation in Macrophages by Inducing NOX-1 Transcription and Rac1 Activation and Suppressing the Expression of Antioxidative Enzymes. *The Journal of Biological Chemistry*, *284*(51), 35403.

Majstoravich, S., Zhang, J., Nicholson-Dykstra, S., Linder, S., Friedrich, W., Siminovitch, K. A., & Higgs, H. N. (2004). Lymphocyte microvilli are dynamic, actin-dependent structures that do not require Wiskott-Aldrich syndrome protein (WASp) for their morphology. *Blood*, *104*(5), 1396–1403.

Mandal, C. C., Ganapathy, S., Gorin, Y., Mahadev, K., Block, K., Abboud, H. E., Harris, S. E., Ghosh-Choudhury, G., & Ghosh-Choudhury, N. (2011). Reactive oxygen species derived from Nox4 mediate BMP2 gene transcription and osteoblast differentiation. *The Biochemical Journal*, *433*(2), 393.

Mao, C., Lei, G., Horbath, A., & Gan, B. (2022). Assessment of lipid peroxidation in irradiated cells. *Methods in Cell Biology*, *172*, 37–50.

Marín-García, J. (2007). Molecular Basis of Lipoprotein Disorders, Atherogenesis, and Thrombosis. *Post-Genomic Cardiology*, 211–260.

Martin, J. G., Suzuki, M., Maghni, K., Pantano, R., Ramos-Barbón, D., Ihaku, D., Nantel, F., Denis, D., Hamid, Q., & Powell, W. S. (2002). The immunomodulatory actions of prostaglandin E2 on allergic airway responses in the rat. *Journal of Immunology (Baltimore, Md. : 1950)*, *169*(7), 3963–3969.

Marzaioli, V., Canavan, M., Floudas, A., Wade, S. C., Low, C., Veale, D. J., & Fearon, U. (2020). Monocyte-Derived Dendritic Cell Differentiation in Inflammatory Arthritis Is Regulated by the JAK/STAT Axis via NADPH Oxidase Regulation. *Frontiers in Immunology*, *11*.

Marzaioli, V., Hurtado-Nedelec, M., Pintard, C., Tlili, A., Marie, J. C., Monteiro, R. C., Gougerot-Pocidalo, M. A., Dang, P. M. C., & El-Benna, J. (2017). NOX5 and p22phox are 2 novel regulators of human monocytic differentiation into dendritic cells. *Blood*, *130*(15), 1734–1745.

McKay, D. M., & MacNaughton, W. K. (2012). Mechanisms and Consequences of Intestinal Inflammation. *Physiology of the Gastrointestinal Tract, Two Volume Set*, 2075–2099.

Minsky, M. (1988). Memoir on inventing the confocal scanning microscope. *Scanning*, *10*(4), 128–138.

Mirjam, K., & Broos, C. E. (2019). Immunological Manifestations in Sarcoidosis. *Sarcoidosis: A Clinician's Guide*, 37–54.

Moghadam, Z. M., Henneke, P., & Kolter, J. (2021). From Flies to Men: ROS and the NADPH Oxidase in Phagocytes. *Frontiers in Cell and Developmental Biology*, *9*, 618.

Møller, I. M., Rogowska-Wrzesinska, A., & Rao, R. S. P. (2011). Protein carbonylation and metal-catalyzed protein oxidation in a cellular perspective. *Journal of Proteomics*, *74*(11), 2228–2242.

Morimoto, H., Kanatsu-Shinohara, M., & Shinohara, T. (2015). ROS-generating oxidase Nox3 regulates the self-renewal of mouse spermatogonial stem cells. *Biology of Reproduction*, *92*(6), 147–148.

Mosser, D. M., & Edwards, J. P. (2008). Exploring the full spectrum of macrophage activation. *Nature Reviews. Immunology*, *8*(12), 958–969.

Mozuraityte, R., Kristinova, V., & Rustad, T. (2016). Oxidation of Food Components. *Encyclopedia of Food and Health*, 186–190.

Nada, M., Ohnishi, H., Tochio, H., Kato, Z., Kimura, T., Kubota, K., Yamamoto, T., Kamatari, Y. O., Tsutsumi, N., Shirakawa, M., & Kondo, N. (2012). Molecular analysis of the binding mode of Toll/interleukin-1 receptor (TIR) domain proteins during TLR2 signaling. *Molecular Immunology*, *52*(3–4), 108–116.

Nadworny, A. S., Guruju, M. R., Poor, D., Doran, R. M., Sharma, R. V., Kotlikoff, M. I., & Davisson, R. L. (2013). Nox2 and Nox4 influence neonatal c-kit+ cardiac precursor cell status and differentiation. *American Journal of Physiology - Heart and Circulatory Physiology*, *305*(6), H829.

Nalobin, D. S., Galiakberova, A. A., Alipkina, S. I., & Glukhov, A. I. (2018). Regulation of Telomerase Activity. *Biology Bulletin Reviews 2018 8:2*, *8*(2), 142–154.

Neumann, C. A., Krause, D. S., Carman, C. V., Das, S., Dubey, D. P., Abraham, J. L., Bronson, R. T., Fujiwara, Y., Orkin, S. H., & Van Etten, R. A. (2003). Essential role for the peroxiredoxin Prdx1 in erythrocyte antioxidant defence and tumour suppression. *Nature*, *424*(6948), 561–565.

Nguyen, G. T., Green, E. R., & Mecsas, J. (2017). Neutrophils to the ROScue: Mechanisms of NADPH Oxidase Activation and Bacterial Resistance. *Frontiers in Cellular and Infection Microbiology*, *7*(AUG).

Nisimoto, Y., Diebold, B. A., Constentino-Gomes, D., & Lambeth, J. D. (2014). Nox4: a hydrogen peroxide-generating oxygen sensor. *Biochemistry*, *53*(31), 5111–5120.

Noguera, A., Batle, S., Miralles, C., Iglesias, J., Busquets, X., MacNee, W., & Agustí, A. G. N. (2001). Enhanced neutrophil response in chronic obstructive pulmonary disease. *Thorax*, *56*(6), 432.

Nunoi, H., Rotrosen, D., Gallin, J. I., & Malech, H. L. (1988). Two forms of autosomal chronic granulomatous disease lack distinct neutrophil cytosol factors. *Science (New York, N.Y.)*, *242*(4883), 1298–1301.

Pagliara, P., Lanubile, R., Dwikat, M., Abbro, L., & Dini, L. (2005). Differentiation of monocytic U937 cells under static magnetic field exposure. *European Journal of Histochemistry : EJH*, *49*(1), 75–86.

Panday, A., Sahoo, M. K., Osorio, D., & Batra, S. (2014). NADPH oxidases: an overview from structure to innate immunity-associated pathologies. *Cellular & Molecular Immunology 2014 12:1*, *12*(1), 5–23.

Park, B. S., & Lee, J. O. (2013). Recognition of lipopolysaccharide pattern by TLR4 complexes. *Experimental & Molecular Medicine*, *45*(12).

Parvez, S., Long, M. J. C., Poganik, J. R., & Aye, Y. (2018). Redox Signaling by Reactive Electrophiles and Oxidants. *Chemical Reviews*, *118*(18), 8798.

Paul, N. E., Skazik, C., Harwardt, M., Bartneck, M., Denecke, B., Klee, D., Salber, J., & Zwadlo-Klarwasser, G. (2008). Topographical control of human macrophages by a regularly microstructured polyvinylidene fluoride surface. *Biomaterials*, *29*(30), 4056–4064.

Peng, C., Li, X., Ao, F., Li, T., Guo, J., Liu, J., Zhang, X., Gu, J., Mao, J., & Zhou, B. (2023). Mitochondrial ROS driven by NOX4 upregulation promotes hepatocellular carcinoma cell survival after incomplete radiofrequency ablation by inducing of mitophagy via Nrf2/PINK1. *Journal of Translational Medicine*, *21*(1).

Pluchino, L. A., & Wang, H. C. R. (2014). Chronic Exposure to Combined Carcinogens Enhances Breast Cell Carcinogenesis with Mesenchymal and Stem-Like Cell Properties. *PLOS ONE*, *9*(11), e108698.

Pospíšil, P., Prasad, A., & Rác, M. (2019). Mechanism of the Formation of Electronically Excited Species by Oxidative Metabolic Processes: Role of Reactive Oxygen Species. *Biomolecules 2019, Vol. 9, Page 258*, *9*(7), 258.

Prasad, A., Kikuchi, H., Inoue, K. Y., Suzuki, M., Sugiura, Y., Sugai, T., Tomonori, A., Tada, M., Kobayashi, M., Matsue, T., & Kasai, S. (2016). Simultaneous real-time monitoring of oxygen consumption and hydrogen peroxide production in cells using our newly developed chip-type biosensor device. *Frontiers in Physiology*, *7*(MAR), 109.

Prasad, A., Kumar, A., Suzuki, M., Kikuchi, H., Sugai, T., Kobayashi, M., Pospíšil, P., Tada, M., & Kasai, S. (2015). Detection of hydrogen peroxide in Photosystem II (PSII) using catalytic amperometric biosensor. *Frontiers in Plant Science*, *6*(OCTOBER), 862.

Prasad, A., Manoharan, R. R., Sedlářová, M., & Pospíšil, P. (2021). Free radical-mediated protein radical formation in differentiating monocytes. *International Journal of Molecular Sciences*, *22*(18), 9963.

Pryor, W. A., & Stanley, J. P. (1975). Letter: A suggested mechanism for the production of malonaldehyde during the autoxidation of polyunsaturated fatty acids. Nonenzymatic production of prostaglandin endoperoxides during autoxidation. *The Journal of Organic Chemistry*, *40*(24), 3615–3617.

Rae, J., Noack, D., Heyworth, P. G., Ellis, B. A., Curnutte, J. T., & Cross, A. R. (2000). Molecular analysis of 9 new families with chronic granulomatous disease caused by mutations in CYBA, the gene encoding p22phox. *Blood*, *96*(3), 1106–1112.

Rots, N. Y., Iavarone, A., Bromleigh, V., & Freedman, L. P. (1999). Induced Differentiation of U937 Cells by 1,25-dihydroxyvitamin D3 Involves Cell Cycle Arrest in G1 That Is Preceded by a Transient Proliferative Burst and an Increase in Cyclin Expression. *Blood*, *93*(8), 2721–2729.

Sahoo, S., Meijles, D. N., & Pagano, P. J. (2016). NADPH oxidases: key modulators in aging and age-related cardiovascular diseases? *Clinical Science (London, England : 1979)*, *130*(5), 317.

Sandison, D. R., & Webb, W. W. (1994). Background rejection and signal-to-noise optimization in confocal and alternative fluorescence microscopes. *Applied Optics, Vol. 33, Issue 4, Pp. 603-615*, *33*(4), 603–615.

Santos, C. X. C., Nabeebaccus, A. A., Shah, A. M., Camargo, L. L., Filho, S. V., & Lopes, L. R. (2014). Endoplasmic Reticulum Stress and Nox-Mediated Reactive Oxygen Species Signaling in the Peripheral Vasculature: Potential Role in Hypertension. *Antioxidants & Redox Signaling*, *20*(1), 121.

Schieber, M., & Chandel, N. S. (2014). ROS function in redox signaling and oxidative stress. *Current Biology : CB*, *24*(10).

Schröder, K., Zhang, M., Benkhoff, S., Mieth, A., Pliquett, R., Kosowski, J., Kruse, C., Luedike, P., Michaelis, U. R., Weissmann, N., Dimmeler, S., Shah, A. M., & Brandes, R. P. (2012). Nox4 Is a protective reactive oxygen species generating vascular NADPH oxidase. *Circulation Research*, *110*(9), 1217–1225.

Sechi, A. S., Wehland, J., & Small, J. V. (1997). The isolated comet tail pseudopodium of Listeria monocytogenes: A tail of two actin filament populations, long and axial and short and random. *Journal of Cell Biology*, *137*(1), 155–167.

Segal, A. W., & Jones, O. T. G. (1978). Novel cytochrome b system in phagocytic vacuoles of human granulocytes. *Nature*, *276*(5687), 515–517.

Segal, A. W., & Jones, O. T. G. (1979). The subcellular distribution and some properties of the cytochrome b component of the microbicidal oxidase system of human neutrophils. *The Biochemical Journal*, *182*(1), 181–188.

Shad, K. F., Das, T. K., Shad, K. F., & Das, T. K. (2023). Introductory Chapter: Role of Fenton and Haber-Weiss Reaction in Epilepsy. *Epilepsy - Seizures without Triggers*.

Sharma, P., Jha, A. B., Dubey, R. S., & Pessarakli, M. (2012). Reactive Oxygen Species, Oxidative Damage, and Antioxidative Defense Mechanism in Plants under Stressful Conditions. *Journal of Botany*, *2012*, 1–26.

Shimada, K., Anai, S., Fujii, T., Tanaka, N., Fujimoto, K., & Konishi, N. (2013). Syndecan-1 (CD138) contributes to prostate cancer progression by stabilizing tumour-initiating cells. *The Journal of Pathology*, *231*(4), 495–504.

Sies, H., Belousov, V. V., Chandel, N. S., Davies, M. J., Jones, D. P., Mann, G. E., Murphy, M. P., Yamamoto, M., & Winterbourn, C. (2022). Defining roles of specific reactive oxygen species (ROS) in cell biology and physiology. *Nature Reviews Molecular Cell Biology 2022 23:7*, *23*(7), 499–515.

Sies, H., Berndt, C., & Jones, D. P. (2017). Oxidative Stress. *Https://Doi.Org/10.1146/Annurev-Biochem-061516-045037*, *86*, 715–748.

Simone, S., Cosola, C., Loverre, A., Cariello, M., Sallustio, F., Rascio, F., Gesualdo, L., Schena, F. P., Grandaliano, G., & Pertosa, G. (2012). BMP-2 induces a profibrotic phenotype in adult renal progenitor cells through Nox4 activation. *American Journal of Physiology. Renal Physiology*, *303*(1). https://doi.org/10.1152/AJPRENAL.00328.2011

Skonieczna, M., Hejmo, T., Poterala-Hejmo, A., Cieslar-Pobuda, A., & Buldak, R. J. (2017). NADPH Oxidases: Insights into Selected Functions and Mechanisms of Action in Cancer and Stem Cells. *Oxidative Medicine and Cellular Longevity*, *2017*.

Snelgrove, R. J., Edwards, L., Rae, A. J., & Hussell, T. (2006). An absence of reactive oxygen species improves the resolution of lung influenza infection. *European Journal of Immunology*, *36*(6), 1364–1373.

Snelgrove, R., Williams, A., Thorpe, C., & Hussell, T. (2004). Manipulation of immunity to and pathology of respiratory infections. *Expert Review of Anti-Infective Therapy*, *2*(3), 413–426.

Spillman, R., Kopaciewicz, W., & Weiss, A. J. (2007). MEMBRANE SEPARATIONS | Membranes in Life Science Applications. *Encyclopedia of Separation Science*, 1–10.

Stephens, T. A., Nikoopour, E., Rider, B. J., Leon-Ponte, M., Chau, T. A., Mikolajczak, S., Chaturvedi, P., Lee-Chan, E., Flavell, R. A., Haeryfar, S. M. M., Madrenas, J., & Singh, B. (2008). Dendritic cell differentiation induced by a self-peptide derived from apolipoprotein E. *Journal of Immunology (Baltimore, Md. : 1950)*, *181*(10), 6859–6871.

Strefford, J. C., Foot, N. J., Chaplin, T., Neat, M. J., Oliver, R. T. D., Young, B. D., & Jones, L. K. (2001). The characterisation of the lymphoma cell line U937, using comparative genomic hybridisation and multi-plex FISH. *Cytogenetics and Cell Genetics*, *94*(1–2), 9–14.

Suh, Y. A., Arnold, R. S., Lassegue, B., Shi, J., Xu, X., Sorescu, D., Chung, A. B., Griendling, K. K., & Lambeth, J. D. (1999). Cell transformation by the superoxide-generating oxidase Mox1. *Nature*, *401*(6748), 79–82.

Suliman, H. B., Ryan, L. K., Bishop, L., & Folz, R. J. (2001). Prevention of influenza-induced lung injury in mice overexpressing extracellular superoxide dismutase. *American Journal of Physiology. Lung Cellular and Molecular Physiology*, *280*(1).

Sun, J., Ming, L., Shang, F., Shen, L., Chen, J., & Jin, Y. (2015). Apocynin suppression of NADPH oxidase reverses the aging process in mesenchymal stem cells to promote osteogenesis and increase bone mass. *Scientific Reports*, *5*.

Sundström, C., & Nilsson, K. (1976). Establishment and characterization of a human histiocytic lymphoma cell line (U-937). *International Journal of Cancer*, *17*(5), 565–577.

Tao, X., & Xu, A. (2016). Basic Knowledge of Immunology. *Amphioxus Immunity: Tracing the Origins of Human Immunity*, 15–42.

Taylor, R. M., Burritt, J. B., Baniulis, D., Foubert, T. R., Lord, C. I., Dinauer, M. C., Parkos, C. A., & Jesaitis, A. J. (2004). Site-specific inhibitors of NADPH oxidase activity and structural probes of flavocytochrome b: characterization of six monoclonal antibodies to the p22phox subunit. *Journal of Immunology (Baltimore, Md. : 1950)*, *173*(12), 7349–7357.

Theivanthiran, B., Batra, S., Balamayooran, G., Cai, S., Kobayashi, K., Flavell, R. A., & Jeyaseelan, S. (2012). NOD2 Signaling Contributes to Host Defense in the Lungs against Escherichia coli Infection. *Infection and Immunity*, *80*(7), 2558.

Therond, P. (2006). [Oxidative stress and damages to biomolecules (lipids, proteins, DNA)]. *Annales Pharmaceutiques Francaises*, *64*(6), 383–389.

Timperi, E., & Ramos, R. N. (2022). Macrophage differentiation. *Macrophages in the Human Body: A Tissue Level Approach*, 19–48.

Topchiy, E., Panzhinskiy, E., Griffin, W. S. T., Barger, S. W., Das, M., & Zawada, W. M. (2013). Nox4-generated superoxide drives angiotensin II-induced neural stem cell proliferation. *Developmental Neuroscience*, *35*(4), 293–305.

Towbin, H., Staehelin, T., & Gordon, J. (1979). Electrophoretic transfer of proteins from polyacrylamide gels to nitrocellulose sheets: procedure and some applications. *Proceedings of the National Academy of Sciences of the United States of America*, *76*(9), 4350–4354.

Trinh, L. A., & Fraser, S. E. (2015). Imaging the Cell and Molecular Dynamics of Craniofacial Development: Challenges and New Opportunities in Imaging Developmental Tissue Patterning. *Current Topics in Developmental Biology*, *115*, 599–629.

Tsai, I. Y., Kuo, C. C., Tomczyk, N., Stachelek, S. J., Composto, R. J., & Eckmann, D. M. (2011). Human macrophage adhesion on polysaccharide patterned surfaces. *Soft Matter*, *7*(7), 3599–3606.

Tuomisto, T. T., Riekkinen, M. S., Viita, H., Levonen, A. L., & Ylä-Herttuala, S. (2005). Analysis of gene and protein expression during monocyte-macrophage differentiation and cholesterol loading--cDNA and protein array study. *Atherosclerosis*, *180*(2), 283–291.

van Furth, R., & Beekhuizen, H. (1998). Monocytes. *Encyclopedia of Immunology*, 1750–1754.

van Furth, R., & Cohn, Z. A. (1968). The origin and kinetics of mononuclear phagocytes. *The Journal of Experimental Medicine*, *128*(3), 415–435.

Vermot, A., Petit-Härtlein, I., Smith, S. M. E., & Fieschi, F. (2021). NADPH Oxidases (NOX): An Overview from Discovery, Molecular Mechanisms to Physiology and Pathology. *Antioxidants 2021, Vol. 10, Page 890*, *10*(6), 890.

Volpp, B. D., Nauseef, W. M., & Clark, R. A. (1988). Two cytosolic neutrophil oxidase components absent in autosomal chronic granulomatous disease. *Science (New York, N.Y.)*, *242*(4883), 1295–1297.

Wada, T., Furuichi, K., Sakai, N., Iwata, Y., Yoshimoto, K., Shimizu, M., Takeda, S. I., Takasawa, K., Yoshimura, M., Kida, H., Kobayashi, K. I., Mukaida, N., Naito, T., Matsushima, K., & Yokoyama, H. (2000). Up-regulation of monocyte chemoattractant protein-1 in tubulointerstitial lesions of human diabetic nephropathy. *Kidney International*, *58*(4), 1492–1499.

Wallner, S., Grandl, M., Konovalova, T., Sigrüner, A., Kopf, T., Peer, M., Orsó, E., Liebisch, G., & Schmitz, G. (2014). Monocyte to Macrophage Differentiation Goes along with Modulation of the Plasmalogen Pattern through Transcriptional Regulation. *PLOS ONE*, *9*(4), e94102.

Wang, Z. R., Cui, Y., & Qiu, Z. Y. (2019). Biomimetic Mineralized Collagen Biocompatibility. *Mineralized Collagen Bone Graft Substitutes*, 61–98.

Wenceslau, C. F., McCarthy, C. G., & Webb, R. C. (2018). To be, or nox to be, endoplasmic reticulum stress in hypertension. *Hypertension*, *72*(1), 59–60.

Wientjes, F. B., Hsuan, J. J., Totty, N. F., & Segal, A. W. (1993). p40phox, a third cytosolic component of the activation complex of the NADPH oxidase to contain src homology 3 domains. *Biochemical Journal*, *296*(Pt 3), 557.

Wu, Y., Antony, S., Juhasz, A., Lu, J., Ge, Y., Jiang, G., Roy, K., & Doroshow, J. H. (2011). Up-regulation and Sustained Activation of Stat1 Are Essential for Interferon-γ (IFN-γ)-induced Dual Oxidase 2 (Duox2) and Dual Oxidase A2 (DuoxA2) Expression in Human Pancreatic Cancer Cell Lines. *The Journal of Biological Chemistry*, *286*(14), 12245.

Xiao, Q., Luo, Z., Pepe, A. E., Margariti, A., Zeng, L., & Xu, Q. (2009). Embryonic stem cell differentiation into smooth muscle cells is mediated by Nox4-produced H2O2. *American Journal of Physiology. Cell Physiology*, *296*(4).

Xie, Y., Kang, R., & Tang, D. (2017). Assessment of Posttranslational Modifications of ATG proteins. *Methods in Enzymology*, *587*, 171–188.

Xue, J., Schmidt, S. V., Sander, J., Draffehn, A., Krebs, W., Quester, I., DeNardo, D., Gohel, T. D., Emde, M., Schmidleithner, L., Ganesan, H., Nino-Castro, A., Mallmann, M. R., Labzin, L., Theis, H., Kraut, M., Beyer, M., Latz, E., Freeman, T. C., … Schultze, J. L. (2014). Transcriptome-based network analysis reveals a spectrum model of human macrophage activation. *Immunity*, *40*(2), 274–288.

Yamamoto, T., Sakaguchi, N., Hachiya, M., Nakayama, F., Yamakawa, M., & Akashi, M. (2008). Role of catalase in monocytic differentiation of U937 cells by TPA: hydrogen peroxide as a second messenger. *Leukemia 2009 23:4*, *23*(4), 761–769.

Yang, C. S., Lee, J. S., Rodgers, M., Min, C. K., Lee, J. Y., Kim, H. J., Lee, K. H., Kim, C. J., Oh, B., Zandi, E., Yue, Z., Kramnik, I., Liang, C., & Jung, J. U. (2012). Autophagy Protein Rubicon Mediates Phagocytic NADPH Oxidase Activation in Response to Microbial Infection or TLR Stimulation. *Cell Host & Microbe*, *11*(3), 264.

Yoshizawa-Ogasawara, A., Ogikubo, S., Satoh, M., Narumi, S., & Hasegawa, T. (2013). Congenital hypothyroidism caused by a novel mutation of the dual oxidase 2 (DUOX2) gene. *Journal of Pediatric Endocrinology and Metabolism*, *26*(1–2), 45–52.

Young, C. N., Cao, X., Guruju, M. R., Pierce, J. P., Morgan, D. A., Wang, G., Iadecola, C., Mark, A. L., & Davisson, R. L. (2012). ER stress in the brain subfornical organ mediates angiotensin-dependent hypertension. *The Journal of Clinical Investigation*, *122*(11), 3960.

Zhang, Z., Duan, Q., Zhao, H., Liu, T., Wu, H., Shen, Q., Wang, C., & Yin, T. (2016). Gemcitabine treatment promotes pancreatic cancer stemness through the Nox/ROS/NF-κB/STAT3 signaling cascade. *Cancer Letters*, *382*(1), 53–63.

Ziegler-Heitbrock, L., Ancuta, P., Crowe, S., Dalod, M., Grau, V., Hart, D. N., Leenen, P. J. M., Liu, Y. J., MacPherson, G., Randolph, G. J., Scherberich, J., Schmitz, J., Shortman, K., Sozzani, S., Strobl, H., Zembala, M., Austyn, J. M., & Lutz, M. B. (2010). Nomenclature of monocytes and dendritic cells in blood. *Blood*, *116*(16).

Zvereva, M. I., Shcherbakova, D. M., & Dontsova, O. A. (2010). Telomerase: Structure, functions, and activity regulation. *Biochemistry (Moscow)*, *75*(13), 1563–1583.